

1 **A genome-wide screen for genes affecting spontaneous direct-repeat recombination in**

2 *Saccharomyces cerevisiae*

3

4

5 Daniele Novarina<sup>\*</sup>, Ridhdhi Desai<sup>†</sup>, Jessica A. Vaisica<sup>†</sup>, Jiongwen Ou<sup>†</sup>, Mohammed Bellaoui<sup>†,1</sup>,

6 Grant W. Brown<sup>†,2</sup> and Michael Chang<sup>\*,3</sup>

7

8 <sup>\*</sup>European Research Institute for the Biology of Ageing, University of Groningen, University

9 Medical Center Groningen, 9713 AV Groningen, the Netherlands

10 <sup>†</sup>Department of Biochemistry and Donnelly Centre, University of Toronto, Toronto, ON M5S

11 3E1, Canada

12

13 <sup>1</sup>Current address: Genetics Unit, Faculty of Medicine and Pharmacy, University Mohammed  
14 Premier, Oujda, Morocco

15

16 <sup>2</sup>Co-corresponding author: Department of Biochemistry and Donnelly Centre, University of

17 Toronto, 160 College Street, Toronto, ON M5S 3E1 Canada. E-mail: [grant.brown@utoronto.ca](mailto:grant.brown@utoronto.ca)

18 <sup>3</sup>Co-corresponding author: European Research Institute for the Biology of Ageing, University of

19 Groningen, University Medical Center Groningen, Antonius Deusinglaan 1, 9713 AV Groningen,

20 the Netherlands. E-mail: [m.chang@umcg.nl](mailto:m.chang@umcg.nl)

21

22 Running title: **Spontaneous recombination screen**

23

24 Keywords:

25 Homologous recombination

26 Direct repeat

27 Functional genomics

28 *Saccharomyces cerevisiae*

29 Genome stability

30 DNA damage

31 DNA repair

32

33

34 ABSTRACT

35  
36 Homologous recombination is an important mechanism for genome integrity maintenance, and  
37 several homologous recombination genes are mutated in various cancers and cancer-prone  
38 syndromes. However, since in some cases homologous recombination can lead to mutagenic  
39 outcomes, this pathway must be tightly regulated, and mitotic hyper-recombination is a hallmark  
40 of genomic instability. We performed two screens in *Saccharomyces cerevisiae* for genes that,  
41 when deleted, cause hyper-recombination between direct repeats. One was performed with the  
42 classical patch and replica-plating method. The other was performed with a high-throughput  
43 replica-pinning technique that was designed to detect low-frequency events. This approach  
44 allowed us to validate the high-throughput replica-pinning methodology independently of the  
45 replicative aging context in which it was developed. Furthermore, by combining the two  
46 approaches, we were able to identify and validate 35 genes whose deletion causes elevated  
47 spontaneous direct-repeat recombination. Among these are mismatch repair genes, the Sgs1-  
48 Top3-Rmi1 complex, the RNase H2 complex, genes involved in the oxidative stress response,  
49 and a number of other DNA replication, repair and recombination genes. Since several of our hits  
50 are evolutionary conserved, and repeated elements constitute a significant fraction of mammalian  
51 genomes, our work might be relevant for understanding genome integrity maintenance in  
52 humans.

53

54

55 INTRODUCTION

56  
57 Homologous recombination (HR) is an evolutionarily conserved pathway that can repair DNA  
58 lesions, including double-strand DNA breaks (DSBs), single-strand DNA (ssDNA) gaps,  
59 collapsed replication forks, and interstrand crosslinks, by using a homologous sequence as the  
60 repair template. HR is essential for the maintenance of genome integrity, and several HR genes  
61 are mutated in human diseases, especially cancers and cancer-prone syndromes (Krejci et al.,  
62 2012; Symington et al., 2014). HR is also required for meiosis (Hunter, 2015) and is important  
63 for proper telomere function (Claussin and Chang, 2015). The yeast *Saccharomyces cerevisiae*  
64 has been a key model organism for determining the mechanisms of eukaryotic recombination.  
65 Our current understanding of the HR molecular pathway comes mainly from the study of DSB  
66 repair. However, most mitotic HR events are likely not due to the repair of DSBs (Claussin et al.,  
67 2017), and can be triggered by diverse DNA structures and lesions, including DNA nicks, ssDNA  
68 gaps, arrested or collapsed replication forks, RNA-DNA hybrids and noncanonical secondary  
69 structures (Symington et al., 2014). An essential intermediate in recombination is ssDNA, which,  
70 in the case of a DSB, is generated by resection of the DSB ends by nucleases. Rad52 stimulates  
71 the loading of Rad51 onto ssDNA, which in turn mediates homologous pairing and strand  
72 invasion, with the help of Rad54, Rad55, and Rad57. After copying the homologous template,  
73 recombination intermediates are resolved with the help of nucleases and helicases, and the HR  
74 machinery is disassembled (Symington et al., 2014).

75 While HR is important for genome integrity, excessive or unregulated recombination in  
76 mitotic cells can be deleterious. Indeed, even though HR is generally considered an error-free  
77 DNA repair pathway, outcomes of HR can be mutagenic. For instance, single strand annealing  
78 (SSA) occurring between direct repeats results in the deletion of the intervening sequence

79 (Bhargava et al., 2016), while recombination between ectopic homolog sequences can lead to  
80 gross chromosomal rearrangements (Heyer, 2015). Mutations and chromosomal aberrations can  
81 be the outcome of recombination between slightly divergent DNA sequences, a process termed  
82 “homeologous recombination” (Spies and Fishel, 2015). Allelic recombination between  
83 homologous chromosomes can lead to loss of heterozygosity (LOH) (Aguilera and García-Muse,  
84 2013). Finally, the copying of the homologous template occurs at lower fidelity than is typical for  
85 replicative DNA polymerases, resulting in mutagenesis (McVey et al., 2016). For these reasons,  
86 the HR process must be tightly controlled, and spontaneous hyper-recombination in mitotic cells  
87 is a hallmark of genomic instability (Aguilera and García-Muse, 2013; Heyer, 2015).

88 Pioneering mutagenesis-based screens led to the identification of hyper-recombination  
89 mutants (Aguilera and Klein, 1988; Keil and McWilliams, 1993). Subsequently, several  
90 systematic screens were performed with the yeast knockout (YKO) collection to identify genes  
91 whose deletion results in a spontaneous hyper-recombinant phenotype. In particular, Alvaro et al.  
92 screened an indirect phenotype, namely elevated spontaneous Rad52 focus formation in diploid  
93 cells, which led to the identification of hyper-recombinant as well as recombination-defective  
94 mutants (Alvaro et al., 2007). A second screen for elevated Rad52 foci in haploid cells identified  
95 additional candidate recombination genes (Styles et al., 2016), although the recombination rates  
96 of these were not assessed directly. A distinct screen of the YKO collection measured elevated  
97 spontaneous LOH events in diploid cells, which arise through recombination between  
98 homologous chromosomes or as a consequence of chromosome loss (Andersen et al., 2008). Here  
99 we describe two systematic genome-scale screens measuring spontaneous recombination in  
100 haploid cells, since the sister chromatid is generally a preferred template for mitotic  
101 recombination relative to the homologous chromosome, both in yeast and mammalian cells  
102 (Johnson and Jasin, 2000; Kadyk and Hartwell, 1992). We use a direct-repeat recombination

103 assay (Smith and Rothstein, 1999), because recombination between direct repeats can have a  
104 significant impact on the stability of mammalian genomes, where tandem and interspersed  
105 repeated elements, such as LINEs and SINEs, are very abundant (George and Alani, 2012;  
106 López-Flores and Garrido-Ramos, 2012).

107       Recombination rate screens were performed both with the classical patch and replica-  
108 plating method and with our recently developed high-throughput replica-pinning technique,  
109 which was designed for high-throughput screens involving low-frequency events (Novarina et al.,  
110 2020). High-throughput replica-pinning is based on the concept that, by robotically pinning an  
111 array of yeast strains many times in parallel, several independent colonies per strain can be  
112 analysed at the same time, giving a semi-quantitative estimate of the rate at which a specific low-  
113 frequency event occurs in each strain. We used both approaches to screen the YKO collection  
114 with the direct-repeat recombination assay. Bioinformatic analysis and direct comparison of the  
115 two screens confirmed the effectiveness of the high-throughput replica-pinning methodology.  
116 Together, we identified and validated 35 genes whose deletion results in elevated spontaneous  
117 direct-repeat recombination, many of which have homologs or functional counterparts in humans.

118

119

## 120 MATERIALS AND METHODS

121

### 122 **Yeast strains and growth conditions**

123 Standard yeast media and growth conditions were used (Sherman, 2002; Treco and Lundblad,  
124 2001). All yeast strains used in this study are derivatives of the BY4741 genetic background  
125 (Brachmann et al., 1998) and are listed in Supporting Information, Table S1.

126

### 127 **Patch and replica-plating screen**

128 To create a recombination assay strain compatible with Synthetic Genetic Array (SGA)  
129 methodology (Kuzmin et al., 2016), the *leu2ΔEcoRI-URA3-leu2ΔBstEII* direct repeat  
130 recombination reporter (Smith and Rothstein, 1999) was introduced into Y5518 by PCR of the  
131 *LEU2* locus from W1479-11C, followed by transformation of Y5518 and selection on SD-ura.  
132 Correct integration was confirmed by PCR, and the resulting strain was designated JOY90.  
133 JOY90 was then crossed to the *MATa* yeast knockout (YKO) collection ((Giaever et al., 2002);  
134 gift of C. Boone, University of Toronto), using SGA methodology (Kuzmin et al., 2016).  
135 Following selection on SD-his-arginine-lysine-uracil+G418+ClonNat+canavanine+thialysine, the  
136 resulting strains have the genotype *MATa xxxΔ::kanMX mfa1Δ::MFA1pr-HIS3*  
137 *leu2ΔEcoRI::URA3-HOcs::leu2ΔBstEII his3Δ1 ura3Δ0 met15Δ0 lyp1Δ can1Δ::natMX*, where  
138 *xxxΔ::kanMX* indicates the YKO gene deletion in each resulting strain.

139 Each YKO strain carrying the recombination reporter was streaked for single colonies on  
140 SD-ura. Single colonies were then streaked in a 1 cm x 1 cm patch on YPD, incubated at 30°C  
141 for 24 h, and then replica-plated to SD-leu to detect recombination events as papillae on the  
142 patch. RDY9 (wild-type) and RDY13 (*elg1Δ::kanMX*; positive control) were included on each  
143 plate. The papillae on SD-leu were scored by visual inspection relative to the control strains,

144 yielding 195 positives (Table S2). The 195 positives were tested in a fluctuation test of 5  
145 independent cultures, and those with a recombination rate of at least  $2 \times 10^{-5}$  (approximately  
146 twofold greater than that of RDY9) were identified (43 strains; Table S2). Positives from the first  
147 fluctuation tests (except *slm3* $\Delta$  and *pex13* $\Delta$ , where rates could not be determined due to the large  
148 numbers of ‘jackpot’ cultures where all colonies had a recombination event) were assayed  
149 further, again with 5 cultures per fluctuation test. Thirty-three gene deletion mutants displayed a  
150 statistically supported increase in recombination rate (Table S2, Figure 1D), using a one-sided  
151 Student’s t-test with a cutoff of  $p=0.05$ .

152

### 153 **Fluctuation tests of spontaneous recombination rates**

154 Fluctuation tests as designed by Luria and Delbrück (Luria and Delbrück, 1943) were performed  
155 by transferring entire single colonies from YPD plates to 4 ml of YPD liquid medium. Cultures  
156 were grown at 30°C to saturation. 100  $\mu$ l of a  $10^5$ -fold dilution were plated on a fully  
157 supplemented SD plate and 200  $\mu$ l of a  $10^2$ -fold dilution were plated on an SD-leu plate. Colonies  
158 were counted after incubation at 30°C for 3 days. The number of recombinant (leu+) colonies per  
159  $10^7$  viable cells was calculated, and the median value was used to determine the recombination  
160 rate by the method of the median (Lea and Coulson, 1949).

161

### 162 **High-throughput replica pinning screen**

163 High-throughput manipulation of high-density yeast arrays was performed with the RoToR-HDA  
164 pinning robot (Singer Instruments). The *MATa* yeast deletion collection (EUROSCARF) was  
165 arrayed in 1536 format (each strain in quadruplicate). The *leu2* $\Delta$ *EcoRI*-*URA3*-*leu2* $\Delta$ *BstEII*  
166 marker to measure direct-repeat recombination (Smith and Rothstein, 1999) was introduced into  
167 the deletion collection through synthetic genetic array (SGA) methodology (Kuzmin et al., 2016)



168 using the JOY90 query strain. The procedure was performed twice in parallel to generate two sets  
169 of the yeast deletion collection containing the *leu2* direct-repeat recombination reporter. Each  
170 plate of each set was then pinned onto six YPD+G418 plates (48 replicates per strain in total),  
171 incubated for one day at 30° and then scanned with a flatbed scanner. Subsequently, each plate  
172 was pinned onto SD-leu solid medium and incubated for two days at 30° to select recombination  
173 events. Finally, all plates were re-pinned on SD-leu solid medium and incubated for one day at  
174 30° before scanning. Colony area measurement was performed using the ImageJ software  
175 package (Schneider et al., 2012) and the ScreenMill Colony Measurement Engine plugin  
176 (Dittmar et al., 2010), to assess colony circularity and size in pixels. Colony data was filtered to  
177 exclude artifacts by requiring a colony circularity score greater than 0.8. Colonies with a pixel  
178 area greater than 50% of the mean pixel area were scored for strains pinned to YPD+G418.  
179 Following replica-pinning to SD-leu, colonies were scored if the pixel area was greater than 10%  
180 of the mean pixel area for the same strain on YPD+G418. For each deletion strain, the ratio of  
181 recombinants (colonies on SD-leu) to total colonies (colonies on YPD+G418) is the  
182 recombination frequency (Table S3). Strains where fewer than 10 colonies grew on YPD+G418  
183 were removed from consideration, as were the 73 YKO collection strains carrying an additional  
184 *msh3* mutation (Lehner et al., 2007). The final filtered data is presented in Table S4.

185

### 186 **Gene Ontology enrichment analysis and functional annotation**

187 GO term analysis was performed using the GO term finder tool (<http://go.princeton.edu/>) using a  
188 P-value cutoff of 0.01 and applying Bonferroni correction, querying biological process  
189 enrichment for each gene set. GO term enrichment results were further processed with REVIGO  
190 (Supek et al., 2011) using the “Medium (0.7)” term similarity filter and simRel score as the  
191 semantic similarity measure. Terms with a frequency greater than 15% in the REVIGO output

192 were eliminated as too general. Gene lists used for the GO enrichment analyses are in Table 1,  
193 and the lists of enriched GO terms obtained are provided in Table S6. Human orthologues in  
194 Table 3 were identified using YeastMine (<https://yeastmine.yeastgenome.org/yeastmine>; accessed  
195 June 25, 2019). Protein-protein interactions were identified using GeneMania  
196 (<https://genemania.org/>; (Warde-Farley et al., 2010)), inputting the 35 validated hyper-rec genes,  
197 and selecting only physical interactions, zero resultant genes, and equal weighting by network.  
198 Network edges were reduced to a single width and nodes were annotated manually using gene  
199 ontology from the *Saccharomyces* Genome Database (<https://www.yeastgenome.org>). Network  
200 annotations were made with the Python implementation of Spatial Analysis of Functional  
201 Enrichment (SAFE) (Baryshnikova, 2016); <https://github.com/baryshnikova-lab/safepy>). The  
202 yeast genetic interaction similarity network and its functional domain annotations were obtained  
203 from (Costanzo et al., 2016). The genetic interaction scores for *YER188W*, *DFG16*, *VMA11*, and  
204 *ABZ2* were downloaded from the Cell Map (<http://thecellmap.org/>; accessed January 9, 2020),

205

## 206 **Statistical analysis**

207 Statistical analysis was performed in Excel or R (<https://cran.r-project.org/>).

208

## 209 **Data availability**

210 Strains are available upon request. A file containing supplemental tables is available at FigShare.

211 Table S1 lists all the strains used in this study. Table S2 contains the fluctuation test data from the  
212 patch screen. Table S3 contains the raw high-throughput replica pinning screen data. Table S4  
213 contains the filtered pinning screen data. Table S5 contains the fluctuation test data from the  
214 pinning screen. Table S6 contains the GO term enrichment data.

215

## 216 RESULTS

217

### 218 **A genetic screen for elevated spontaneous direct-repeat recombination**

219 The *leu2* direct-repeat recombination assay (Smith and Rothstein, 1999) can detect both intra-  
220 chromosomal and sister chromatid recombination events (Figure 1A). Two nonfunctional *leu2*  
221 heteroalleles are separated by a 5.3 kb region containing the *URA3* marker. Reconstitution of a  
222 functional *LEU2* allele can occur either via sister chromatid recombination (gene conversion),  
223 which maintains the *URA3* marker, or via intra-chromosomal SSA, with the concomitant deletion  
224 of the sequence between the direct repeats and subsequent loss of the *URA3* marker (Symington  
225 et al., 2014). Both recombination events can be selected on media lacking leucine. We used this  
226 assay to systematically screen the yeast knockout (YKO) collection for genes whose deletion  
227 results in hyper-recombination between direct repeats (Figure 1B). We introduced the *leu2* direct-  
228 repeat recombination reporter into the YKO collection via synthetic genetic array (SGA)  
229 technology (Kuzmin et al., 2016). Each of the ~4500 obtained strains was then patched on non-  
230 selective plates and replica-plated to plates lacking leucine to detect spontaneous recombination  
231 events as papillae on the replica-plated patches (Figure 1C). We included a wild-type control and  
232 a hyper-recombinant *elg1Δ* control (Bellaoui et al., 2003; Ben-Aroya et al., 2003) on every plate  
233 for reference. The recombination rates for 195 putative hyper-rec mutants identified by replica-  
234 plating (Table S2) were measured by a fluctuation test. Strains with a recombination rate greater  
235 than  $2 \times 10^{-5}$  (approximately twofold of the wild-type rate; 38 strains) were assayed in triplicate (or  
236 more). Thirty-three gene deletion mutant strains with a statistically supported increase in direct-  
237 repeat recombination rate relative to the wild-type control were identified (Figure 1D, Table S2,  
238 Table 1). The genes identified showed a high degree of enrichment for GO terms reflecting roles  
239 in DNA replication and repair (Figure 1E).

240

## 241 **A high-throughput screen for altered spontaneous direct-repeat recombination**

242 We recently developed a high-throughput replica-pinning method to detect low-frequency events,  
243 and validated the scheme in a genome-scale mutation frequency screen (Novarina et al., 2020).

244 To complement the data obtained with the classical screening approach, and to test our new  
245 methodology independently of the replicative aging context in which it was developed, we

246 applied it to detect changes in spontaneous direct-repeat recombination (Figure 2A). We again  
247 introduced the *leu2* direct-repeat recombination reporter (Figure 1A) into the YKO collection.

248 The collection was then amplified by parallel high-throughput replica-pinning to yield 48

249 colonies per gene deletion strain. After one day of growth, all colonies were replica-pinned

250 (twice, in series) to media lacking leucine to select for recombination events. Recombination

251 frequencies (a proxy for the spontaneous recombination rate) were calculated for each strain of

252 the collection (Figure 2B, Table S3, Table S4). As a reference, recombination frequencies for the

253 wild type (46%) and for a recombination-deficient *rad54*Δ strain (21%) obtained in a pilot

254 replica-pinning experiment of 3000 colonies are indicated. In the screen itself, where 48 colonies

255 were assessed, the wild type (*his3*Δ::*kanMX*) had a recombination frequency of 56%. Notably, a

256 group of strains from the YKO collection carry an additional mutation in the mismatch repair

257 gene *MSH3* (Lehner et al., 2007). Given the elevated spontaneous recombination rates of several

258 mismatch repair-deficient strains (Figure 1D), we suspected that these *msh3* strains would display

259 increased recombination frequencies, independently of the identity of the intended gene deletion.

260 Indeed, the distribution of recombination frequencies for *msh3* strains (median: 74%) is shifted

261 toward higher values compared to the overall distribution of the YKO collection (median: 60%)

262 (Figure 2B). The 73 *msh3* strains were excluded from further analysis.

263 To explore the overall quality of the high-throughput replica-pinning screen and to  
264 determine a cutoff in an unbiased manner, we performed Cutoff Linked to Interaction Knowledge  
265 (CLIK) analysis (Dittmar et al., 2013). The CLIK algorithm identified an enrichment of highly  
266 interacting genes at the top and at the bottom of our gene list (ranked according to recombination  
267 frequency), confirming the overall high quality of our screen, and indicating that we were able to  
268 detect both hyper- and hypo-recombinogenic mutants (Figure 2C). The cutoff indicated by CLIK  
269 corresponds to a recombination frequency of 87% for the hyper-recombination strains (75 genes;  
270 Table 1), and of 33% for the recombination-deficient strains (122 genes; Table 2).

271  
272 *Hyper-recombination genes.* We assessed the functions of the 75 hyper-recombination genes  
273 identified by our high-throughput screen (Figure 2D). As with the genes identified in the patch  
274 screen, the genes identified in the pinning screen were enriched for DNA replication and repair  
275 functions. Most importantly, at the very top of our hyper-recombination gene list (with 96% to  
276 100% recombination), 11 out of 13 genes were identified in the patch screen and validated by  
277 fluctuation analysis (Table S2). We tested the two additional genes, *CSMI* and *NUP170*, by  
278 fluctuation analysis, and found that both had a statistically supported increase in recombination  
279 rate (Figure 2E and Table S5). Eighteen validated hyper-recombination genes from the patch  
280 screen were not identified in the pinning screen, and so are false negatives. Although we have not  
281 validated the weaker hits from the pinning screen (those with recombination frequencies between  
282 87% and 96%), four genes in this range were validated as part of the patch screen (*APNI*, *RMII*,  
283 *YLR235C*, and *RNH201*), 9 caused elevated levels of Rad52 foci when deleted (*APNI*, *NFII*,  
284 *RMII*, *POL32*, *RNH201*, *DDC1*, *HST3*, *MFT1*, and *YJR124C*) (Alvaro et al., 2007; Styles et al.,  
285 2016), and 3 are annotated as ‘mitotic recombination increased’ (*RMII*, *DDC1*, and *HST3*;

286 *Saccharomyces* Genome Database). Together these data suggest that additional bona fide hyper-  
287 recombination genes were identified in the pinning screen.

288  
289 *Hypo-recombination genes.* By contrast to the replica-plating screen, the pinning screen detected  
290 mutants with reduced recombination frequency, with 122 genes identified (Table 2). The genes  
291 identified were functionally diverse, with no gene ontology (GO) processes enriched. Only 19  
292 nonessential genes are annotated as having reduced recombination as either null or hypomorphic  
293 alleles in the *Saccharomyces* genome database (SGD; accessed January 11, 2020 via YeastMine).  
294 Of these, three genes (*RAD52*, *LRP1*, and *THP1*) were detected in the pinning screen. In addition,  
295 other members of the *RAD52* epistasis group important for effective homologous recombination  
296 (*RAD50*, *RAD54* and *RAD55*) displayed a recombination frequency lower than 33%, and *RAD51*  
297 was just above the cutoff (Table S3). Thus, our high-throughput replica-pinning approach detects  
298 mutants with very low recombination frequencies. More generally, this observation suggests that  
299 if the pinning procedure is properly calibrated, a high-throughput replica-pinning screen is able  
300 not only to detect mutants with increased rates of a specific low-frequency event (in this case  
301 direct-repeat recombination), but also mutants with reduced rates of the same low-frequency  
302 event.

303  
304 *Validated hyper-recombination genes identified in both screens.* We compared the genes  
305 identified in the pinning screen with those identified in the patch screen, revealing 15 genes that  
306 were identified in both screens, a statistically supported enrichment (Figure 3A; hypergeometric  $p$   
307 =  $1.2 \times 10^{-21}$ ). Combining the results of the two screens, we validated 35 genes whose deletion  
308 results in elevated spontaneous direct-repeat recombination (Table 3). Analysis of the group of 35  
309 hyper-rec genes revealed 68 pairwise protein-protein interactions (Figure 3B), with many cases

310 where several (if not all) members of the particular protein complex were identified. We found  
311 that 29 of the hyper-rec genes had at least one human orthologue (Table 3), indicating a high  
312 degree of conservation across the 35 validated genes. To assess the functional properties of the 35  
313 gene hyper-rec set, we applied spatial analysis of functional enrichment (SAFE) (Baryshnikova,  
314 2016) to determine if any regions of the functional genetic interaction similarity yeast cell map  
315 (Costanzo et al., 2016) are over-represented for the hyper-rec gene set (Figure 3C). We found a  
316 statistically supported over-representation of the hyper-rec genes in the DNA replication and  
317 repair neighbourhood of the genetic interaction cell map, highlighting the importance of accurate  
318 DNA synthesis in suppressing recombination. Finally, we compared the validated hyper-rec  
319 genes to relevant functional genomic instability datasets (*Saccharomyces* Genome Database  
320 annotation, (Alvaro et al., 2007; Hendry et al., 2015; Stirling et al., 2011; Styles et al., 2016);  
321 Figure 3D). Eight of our hyper-rec genes (*HTA2*, *MSH6*, *YER188W*, *ABZ2*, *PMS1*, *MSH2*,  
322 *DFG16*, and *VMA11*) were not identified in these datasets, indicating that our screens identified  
323 uncharacterized recombination genes. *HTA2*, *MSH6*, *PMS1*, *MSH2* have recombination  
324 phenotypes reported (see Discussion). Thus, we identify four genes without a characterized role  
325 in preventing recombination: *YER188W*, *ABZ2*, *DFG16*, and *VMA11*.

326  
327 To infer gene function for the four genes lacking a characterized role in suppressing  
328 recombination, we again applied SAFE analysis (Baryshnikova, 2016) to annotate the functional  
329 genetic interaction similarity yeast cell map (Costanzo et al., 2016) to identify any regions that  
330 are enriched for genetic interactions with each of the four genes (Figure 4). Of particular interest,  
331 the mitochondrial functional neighbourhood is enriched for negative genetic interactions with  
332 *YER188W* (Figure 4), suggesting that deletion of *YER188W* confers sensitivity to mitochondrial  
333 dysfunction. Analysis of *DFG16* revealed enrichments for positive interactions in the RIM

334 signaling neighbourhood, which is expected (Barwell et al., 2005), but also for negative  
335 interactions in the DNA replication region of the map (Figure 4), indicating that *DFG16* is  
336 important for fitness when DNA replication is compromised. Analysis of *VMA11* revealed  
337 enrichment in the vesicle trafficking neighbourhood, typical of vacuolar ATPase subunit genes,  
338 and analysis of *ABZ2* revealed little (Figure 4). We conclude that functional analysis suggests  
339 mechanisms by which loss of *YER188W* (oxidative stress) or *DFG16* (genome integrity) results  
340 in hyper-recombination.

341

## 342 DISCUSSION

343 Here we briefly discuss the functions of the genes and complexes identified in the screens and  
344 subsequently validated by fluctuation analysis.

345 **Mismatch repair:** *MLH1*, *MSH2*, *MSH6* and *PMS1* are evolutionary conserved genes involved in  
346 mismatch repair (MMR), a pathway that detects and corrects nucleotide mismatches in double-  
347 strand DNA (Spies and Fishel, 2015). An anti-recombinogenic role for these four MMR genes in  
348 yeast has been previously described: specifically, MMR proteins are important to prevent  
349 homeologous recombination and SSA between slightly divergent sequences, via mismatch  
350 recognition and heteroduplex rejection (Datta et al., 1996; Nicholson et al., 2000; Spies and  
351 Fishel, 2015; Sugawara et al., 2004). The role for MMR in preventing homeologous  
352 recombination is conserved also in mammalian cells (de Wind et al., 1995; Elliott and Jasin,  
353 2001; Spies and Fishel, 2015). It is worth noting that the presence of sequence differences  
354 between the two *leu2* alleles in the *leu2* direct-repeat assay is essential to genetically detect  
355 recombination events. Therefore, it is reasonable that this assay should detect genes involved in  
356 suppressing homeologous recombination.

357



358 ***Sgs1-Top3-Rmi1 complex:*** The evolutionary conserved helicase-topoisomerase complex Sgs1-  
359 Top3-Rmi1 is involved in DSB resection and in dissolution of recombination intermediates  
360 (Symington et al., 2014). Consistent with previous observations (Chang et al., 2005), our screen  
361 identified all three members of the complex, together with *YLR235C*, a dubious ORF that  
362 overlaps the *TOP3* gene. The Sgs1-Top3-Rmi1 complex dissolves double Holliday junction  
363 structures to prevent crossover formation (Cejka et al., 2010). The same role has been reported  
364 for BLM helicase, the human Sgs1 homolog mutated in the genome stability disorder Bloom  
365 syndrome (Wu et al., 2006; Yang et al., 2010). Furthermore, several genetic studies indicate that  
366 the anti-recombinogenic activity of Sgs1-Top3-Rmi1 cooperates with MMR proteins in  
367 heteroduplex rejection to prevent homeologous recombination (Chakraborty et al., 2016;  
368 Goldfarb and Alani, 2005; Myung et al., 2001; Spell and Jinks-Robertson, 2004; Sugawara et al.,  
369 2004).

370  
371 ***MGS1:*** In our screen we also identified *MGS1*, the homolog of the WRN-interacting protein  
372 WRNIP1. Mgs1 displays DNA-dependent ATPase and DNA strand annealing activities. Deletion  
373 of *MGS1* causes hyper-recombination, including elevated direct-repeat recombination (Hishida et  
374 al., 2001). It seems that Mgs1 promotes faithful DNA replication by regulating Pol $\delta$ , and  
375 promoting replication fork restart after stalling (Branzei et al., 2002; Saugar et al., 2012). The  
376 absence of Mgs1 could result in increased replication fork collapse, leading to the formation of  
377 recombinogenic DSBs (Branzei et al., 2002). Similar roles have been suggested for WRNIP1 in  
378 mammalian cells (Leuzzi et al., 2016; Tsurimoto et al., 2005).

379  
380 ***RNase H2 complex:*** *RNH201* encodes the evolutionary conserved catalytic subunit of RNase H2,  
381 while the two non-catalytic subunits are encoded by *RNH202* and *RNH203* genes. This enzyme

382 cleaves the RNA moiety in RNA-DNA hybrids originating from Okazaki fragments, co-  
383 transcriptional R-loops, and ribonucleotide incorporation by replicative polymerases (Cerritelli  
384 and Crouch, 2009). Deletion of any of the three subunits in yeast inactivates the whole complex.  
385 Human RNase H2 genes are mutated in Aicardi-Goutières syndrome, a severe neurological  
386 disorder (Crow et al., 2006). Inactivation of yeast RNase H2 causes elevated LOH, ectopic  
387 recombination and direct-repeat recombination (Conover et al., 2015; Potenski et al., 2014),  
388 mostly dependent on Top1 activity. What is the recombinogenic intermediate accumulated in the  
389 absence of RNase H2? It has been suggested that Top1-dependent cleavage at the ribonucleotide  
390 site creates a nick that can be further converted into a recombinogenic DSB (Potenski et al.,  
391 2014). Recent genetic studies indicate that, while in the case of LOH events hyper-recombination  
392 is caused by Top1-dependent processing of single ribonucleotides incorporated by leading strand  
393 polymerases and/or by accumulation of recombinogenic R-loops (Conover et al., 2015; Cornelio  
394 et al., 2017; Keskin et al., 2014; O'Connell et al., 2015), elevated direct-repeat recombination  
395 results instead from Top1-dependent cleavage of stretches of ribonucleotides, resulting from  
396 defective R-loop removal or Okazaki fragment processing in the absence of RNase H2 (Epshtein  
397 et al., 2016). In line with this model, we also detected elevated direct-repeat recombination rate in  
398 the absence of the Thp2 member of the THO complex, which functions at the interface between  
399 transcription and mRNA export to prevent R-loop accumulation (Chavez et al., 2000; Huertas  
400 and Aguilera, 2003), *DST1*, which encodes a transcription elongation factor and is anti-  
401 recombinogenic (Owiti et al., 2017), and the flap endonuclease encoded by *RAD27*, which is  
402 involved in Okazaki fragment processing (Balakrishnan and Bambara, 2013) (Table 3).  
403 Furthermore, deletion of the dubious ORF *YDL162C*, also identified in our screen, likely affects  
404 the expression level of neighbouring *CDC9*, an essential gene encoding DNA Ligase I, involved  
405 in Okazaki fragment processing and ligation after ribonucleotide removal from DNA. Together,

406 available data suggest that different modes leading to accumulation of RNA-DNA hybrids or  
407 unprocessed Okazaki fragments result in hyper-recombination.

408  
409 ***Fork protection complex:*** Tof1 and Csm3 (Timeless and Tipin in human cells) form the fork  
410 protection complex (FPC), involved in stabilization of replication forks, maintenance of sister  
411 chromatid cohesion and DNA replication checkpoint signaling (Bando et al., 2009; Chou and  
412 Elledge, 2006; Katou et al., 2003; Leman et al., 2010; Mayer et al., 2004; Mohanty et al., 2006;  
413 Noguchi et al., 2004, 2003; Xu et al., 2004). Recently, Tof1 and Csm3 were implicated in  
414 restricting fork rotation genome-wide during replication; they perform this role independently of  
415 their interacting partner Mrc1, which we did not identify in our screen (Schalbetter et al., 2015).  
416 In the absence of Tof1 or Csm3, excessive fork rotation can cause spontaneous DNA damage, in  
417 the form of recombinogenic ssDNA and DSBs (Chou and Elledge, 2006; Schalbetter et al., 2015;  
418 Sommariva et al., 2005; Urtishak et al., 2009). Indeed, depletion of Tof1 and Csm3 orthologues  
419 results in accumulation of recombination intermediates in fission yeast and mouse cells (Noguchi  
420 et al., 2004, 2003; Sommariva et al., 2005; Urtishak et al., 2009).

421  
422 ***RRM3:*** The *RRM3* gene, encoding a 5' to 3' DNA helicase, was initially identified because its  
423 absence causes hyper-recombination between endogenous tandem-repeated sequences (such as  
424 the rDNA locus and the *CUP1* genes) (Keil and McWilliams, 1993). The Rrm3 helicase travels  
425 with the replication fork and facilitates replication through genomic sites containing protein-DNA  
426 complexes that, in its absence, cause replication fork stalling and breakage. Such Rrm3-  
427 dependent sites include the rDNA, telomeres, tRNA genes, inactive replication origins,  
428 centromeres, and the silent mating-type loci (Azvolinsky et al., 2006; Ivessa et al., 2003, 2000;

429 Schmidt and Kolodner, 2004; Torres et al., 2004). Intriguingly, a tRNA gene is located about 350  
430 bp upstream the chromosomal location of the *leu2* direct-repeat recombination marker. Increased  
431 replication fork pausing in the absence of Rrm3 could cause recombinogenic DSBs, explaining  
432 the elevated direct-repeat recombination we observe in the *rrm3Δ* strain.

433  
434 ***Oxidative stress response genes:*** *YAP1* and *SKN7* encode two transcription factors important for  
435 the activation of the cellular response to oxidative stress (Morano et al., 2012). The glutathione  
436 peroxidase encoded by *HYR1* has a major role in activating Yap1 in response to oxidative stress  
437 (Delaunay et al., 2002). *TSA1* is a Yap1 and Skn7 target and encodes a peroxiredoxin that  
438 scavenges endogenous hydrogen peroxide (Wong et al., 2004). Deletion of *TSA1* causes hyper-  
439 recombination between inverted repeats (Huang and Kolodner, 2005), and oxidative stress  
440 response genes (including *TSA1*, *SKN7* and *YAP1*) are synthetic sick or lethal with HR mutants  
441 (Pan et al., 2006; Yi et al., 2016). A likely explanation for the elevated direct-repeat  
442 recombination we measured in strains defective for the oxidative stress response, therefore, is that  
443 oxidative DNA damage generates replication blocking lesions and/or replication-associated  
444 DSBs, both of which are processed by the HR pathway (Huang and Kolodner, 2005). An  
445 alternative explanation could be that extensive oxidative DNA damage results in the saturation of  
446 the mismatch-binding step of MMR, compromising MMR-dependent heteroduplex rejection,  
447 resulting in increased homeologous recombination (Hum and Jinks-Robertson, 2018; Spies and  
448 Fishel, 2015).

449  
450 ***Other DNA Repair genes:*** *APN1* encodes the main apurinic/aprimidinic (AP) endonuclease  
451 involved in yeast base excision repair (BER). Removal of endogenous alkylating damage can  
452 generate abasic sites, which are mostly processed by Apn1 (Boiteux and Guillet, 2004; Popoff et

453 al., 1990; Xiao and Samson, 1993). In the absence of *APNI*, abasic sites accumulate, which can  
454 hamper DNA replication. The recombination pathway is involved in the repair and/or bypass of  
455 these abasic sites, as suggested by the genetic interactions between the BER and the HR  
456 pathways (Boiteux and Guillet, 2004; Swanson et al., 1999; Vance and Wilson, 2001). The *APNI*  
457 gene is adjacent to *RAD27*, and therefore it is also possible that the hyper-recombination  
458 phenotype of *apn1Δ* is due to a “neighbouring-gene effect” on *RAD27*, as was reported in the  
459 case of telomere length alteration (Ben-Shitrit et al., 2012).

460 *HTA2*, which encodes one copy of histone H2A, is of course important for appropriate  
461 nucleosome assembly. Reducing histone levels by deleting one H3-H4 gene pair or by partial  
462 depletion of H4 increases recombination (Clemente-Ruiz and Prado, 2009; Liang et al., 2012;  
463 Prado and Aguilera, 2005), and it is likely that reducing *HTA2* gene dosage also does so. Since  
464 histone depletion results in diverse chromatin defects, the exact mechanisms by which  
465 recombination is induced are elusive.

466 *RAD4* encodes a key factor of nucleotide excision repair (NER), and is involved in direct  
467 recognition and binding of DNA damage (Prakash and Prakash, 2000), while *RAD6* is a key gene  
468 controlling the post replication repair (PRR) DNA damage tolerance pathway (Ulrich, 2005).  
469 Genetic studies suggest that BER, NER, PRR and HR can redundantly process spontaneous DNA  
470 lesions, and inactivation of one pathway shifts the burden on the others. This mechanism could  
471 explain why deletion of *RAD4* or *RAD6* causes a modest increase in spontaneous direct-repeat  
472 recombination (Swanson et al., 1999).

473 *CSMI* encodes a nucleolar protein that serves as a kinetochore organizer to promote  
474 chromosome segregation in meiosis, and is involved in localization and silencing of rDNA and  
475 telomeres in mitotic cells (Poon and Mekhail, 2011). Interestingly, Csm1 is important to inhibit  
476 homologous recombination at the rDNA locus and other repeated sequences (Burrack et al.,

477 2013; Huang et al., 2006; Mekhail et al., 2008). The nuclear pore complex has an intimate  
478 connection to recombination, in that some DSBs move to and are likely repaired at the NPC  
479 (Freudenreich and Su, 2016). The NPC gene *NUP170* has not been directly implicated in DSB  
480 repair, but is important for chromosome segregation (Kerscher et al., 2001).

481  
482 ***The unknowns (YER188W, ABZ2, DFG16, and VMA11):*** Unexpectedly, the top hyper-rec gene  
483 identified in our screen is *VMA11*, which encodes a subunit of the evolutionarily conserved  
484 vacuolar H<sup>+</sup>-ATPase (V-ATPase), important for vacuole acidification and cellular pH regulation  
485 (Hirata et al., 1997; Kane, 2006; Umemoto et al., 1991). *VMA11* involvement in genome  
486 maintenance is suggested by the sensitivity of a *vma11Δ* strain to several genotoxic agents,  
487 namely doxorubicin, ionizing radiation, cisplatin and oxidative stress (Thorpe et al., 2004; Xia et  
488 al., 2007). V-ATPase defects in yeast result in endogenous oxidative stress and defective Fe/S  
489 cluster biogenesis as a consequence of mitochondrial depolarization (Hughes and Gottschling,  
490 2012; Milgrom et al., 2007; Veatch et al., 2009). Of note, several DNA replication and repair  
491 factors are Fe/S cluster proteins (Veatch et al., 2009; Zhang, 2014). Therefore, the hyper-  
492 recombination phenotype of *vma11Δ* could be due to increased spontaneous DNA damage,  
493 caused by elevated endogenous oxidative stress and/or by defective DNA replication and repair  
494 as a consequence of compromised Fe/S cluster biogenesis. However, *VMA11* was not detected in  
495 screens for increased Rad52 foci (Alvaro et al., 2007; Styles et al., 2016), or in a screen for  
496 increased DNA damage checkpoint activation (Hendry et al., 2015), suggesting that spontaneous  
497 DNA damage might not accumulate to high levels in *vma11Δ*.

498 *ABZ2* encodes an enzyme involved in folate biosynthesis (Botet et al., 2007). Folate  
499 deficiency and the resulting compromise of nucleotide synthesis could promote recombination,  
500 although yeast culture media are rich in folate, and the *ABZ2* genetic interaction profile reveals

501 no similarity to nucleotide biosynthesis genes (Usaj et al., 2017). *DFGI6* encodes a predicted  
502 transmembrane protein involved in pH sensing (Barwell et al., 2005). Interestingly, SAFE  
503 analysis indicates a role for *DFGI6* in DNA replication and/or DNA repair, in addition to the  
504 expected role in pH signaling. There is currently little insight into the function of *YERI88W*.  
505 SAFE analysis indicates a possible role in mitochondrial function, however a protein product of  
506 *YERI88W* has not been detected to date in either mass spectrometry or GFP fusion protein  
507 analyses (Breker et al., 2014; Ho et al., 2018; Huh et al., 2003).

508

#### 509 ACKNOWLEDGMENTS

510 We thank Anastasia Baryshnikova for advice and assistance with the SAFE analysis. This work  
511 was supported by grants from the Netherlands Organisation for Scientific Research (Vidi grant  
512 864.12.002 to MC) and the Canadian Institutes of Health Research (MOP-79368 and FDN-  
513 159913 to GWB).

514

515

516 LITERATURE CITED

- 517 Aguilera, A., García-Muse, T., 2013. Causes of genome instability. *Annu. Rev. Genet.* 47, 1–32.  
518 <https://doi.org/10.1146/annurev-genet-111212-133232>
- 519 Aguilera, A., Klein, H.L., 1988. Genetic control of intrachromosomal recombination in  
520 *Saccharomyces cerevisiae*. I. Isolation and genetic characterization of hyper-recombination  
521 mutations. *Genetics* 119, 779–790.
- 522 Alvaro, D., Lisby, M., Rothstein, R., 2007. Genome-wide analysis of Rad52 foci reveals diverse  
523 mechanisms impacting recombination. *PLoS Genet.* 3, 2439–2449.  
524 <https://doi.org/10.1371/journal.pgen.0030228>
- 525 Andersen, M.P., Nelson, Z.W., Hetrick, E.D., Gottschling, D.E., 2008. A genetic screen for  
526 increased loss of heterozygosity in *Saccharomyces cerevisiae*. *Genetics* 179, 1179–1195.  
527 <https://doi.org/10.1534/genetics.108.089250>
- 528 Azvolinsky, A., Dunaway, S., Torres, J.Z., Bessler, J.B., Zakian, V.A., 2006. The *S. cerevisiae*  
529 Rrm3p DNA helicase moves with the replication fork and affects replication of all yeast  
530 chromosomes. *Genes Dev.* 20, 3104–3116. <https://doi.org/10.1101/gad.1478906>
- 531 Balakrishnan, L., Bambara, R.A., 2013. Flap Endonuclease 1. *Annu. Rev. Biochem.* 82, 119–138.  
532 <https://doi.org/10.1146/annurev-biochem-072511-122603>
- 533 Bando, M., Katou, Y., Komata, M., Tanaka, H., Itoh, T., Sutani, T., Shirahige, K., 2009. Csm3,  
534 Tof1, and Mrc1 form a heterotrimeric mediator complex that associates with DNA  
535 replication forks. *J. Biol. Chem.* 284, 34355–34365.  
536 <https://doi.org/10.1074/jbc.M109.065730>
- 537 Barwell, K.J., Boysen, J.H., Xu, W., Mitchell, A.P., 2005. Relationship of *DFG16* to the  
538 Rim101p pH response pathway in *Saccharomyces cerevisiae* and *Candida albicans*.  
539 *Eukaryot. Cell* 4, 890–899. <https://doi.org/10.1128/ec.4.5.890-899.2005>
- 540 Baryshnikova, A., 2018. Spatial analysis of functional enrichment (SAFE) in large biological  
541 networks. *Methods Mol. Biol.* 1819, 249–268. [https://doi.org/10.1007/978-1-4939-8618-7\\_12](https://doi.org/10.1007/978-1-4939-8618-7_12)  
542 7\_12
- 543 Baryshnikova, A., 2016. Systematic functional annotation and visualization of biological  
544 networks. *Cell Syst.* 2, 412–421. <https://doi.org/10.1016/j.cels.2016.04.014>
- 545 Bellaoui, M., Chang, M., Ou, J., Xu, H., Boone, C., Brown, G.W., 2003. Elg1 forms an  
546 alternative RFC complex important for DNA replication and genome integrity. *EMBO J.* 22,  
547 4304–4313. <https://doi.org/10.1093/emboj/cdg406>
- 548 Ben-Aroya, S., Koren, A., Liefshitz, B., Steinlauf, R., Kupiec, M., 2003. *ELG1*, a yeast gene  
549 required for genome stability, forms a complex related to replication factor C. *Proc. Natl.*  
550 *Acad. Sci. U. S. A.* 100, 9906–9911. <https://doi.org/10.1073/pnas.1633757100>
- 551 Ben-Shitrit, T., Yosef, N., Shemesh, K., Sharan, R., Ruppin, E., Kupiec, M., 2012. Systematic  
552 identification of gene annotation errors in the widely used yeast mutation collections. *Nat.*



- 553       Methods 9, 373–378. <https://doi.org/10.1038/nmeth.1890>
- 554       Bhargava, R., Onyango, D.O., Stark, J.M., 2016. Regulation of single-strand annealing and its  
555       role in genome maintenance. *Trends Genet.* 32, 566–575.  
556       <https://doi.org/10.1016/j.tig.2016.06.007>
- 557       Boiteux, S., Guillet, M., 2004. Abasic sites in DNA: Repair and biological consequences in  
558       *Saccharomyces cerevisiae*. *DNA Repair (Amst)*. 3, 1–12.  
559       <https://doi.org/10.1016/j.dnarep.2003.10.002>
- 560       Botet, J., Mateos, L., Revuelta, J.L., Santos, M.A., 2007. A chemogenomic screening of  
561       sulfanilamide-hypersensitive *Saccharomyces cerevisiae* mutants uncovers *ABZ2*, the gene  
562       encoding a fungal aminodeoxychorismate lyase. *Eukaryot. Cell* 6, 2102–2111.  
563       <https://doi.org/10.1128/ec.00266-07>
- 564       Brachmann, C.B., Davies, A., Cost, G.J., Caputo, E., Li, J., Hieter, P., Boeke, J.D., 1998.  
565       Designer deletion strains derived from *Saccharomyces cerevisiae* S288C: a useful set of  
566       strains and plasmids for PCR-mediated gene disruption and other applications. *Yeast* 14,  
567       115–132. [https://doi.org/10.1002/\(SICI\)1097-0061\(19980130\)14:2<115::AID-](https://doi.org/10.1002/(SICI)1097-0061(19980130)14:2<115::AID-YEA204>3.0.CO;2-2)  
568       YEA204>3.0.CO;2-2
- 569       Branzei, D., Seki, M., Onoda, F., Enomoto, T., 2002. The product of *Saccharomyces cerevisiae*  
570       *WHIP/MGS1*, a gene related to replication factor C genes, interacts functionally with DNA  
571       polymerase  $\delta$ . *Mol. Genet. Genomics* 268, 371–386. [https://doi.org/10.1007/s00438-002-](https://doi.org/10.1007/s00438-002-0757-3)  
572       0757-3
- 573       Breker, M., Gymrek, M., Moldavski, O., Schuldiner, M., 2014. LoQAtE - Localization and  
574       Quantitation ATlas of the yeast proteomE. A new tool for multiparametric dissection of  
575       single-protein behavior in response to biological perturbations in yeast. *Nucleic Acids Res.*  
576       42, D726–D730. <https://doi.org/10.1093/nar/gkt933>
- 577       Burrack, L.S., Applen Clancey, S.E., Chacon, J.M., Gardner, M.K., Berman, J., 2013. Monopolin  
578       recruits condensin to organize centromere DNA and repetitive DNA sequences. *Mol. Biol.*  
579       Cell. <https://doi.org/10.1091/mbc.e13-05-0229>
- 580       Cejka, P., Plank, J.L., Bachrati, C.Z., Hickson, I.D., Kowalczykowski, S.C., 2010. Rmi1  
581       stimulates decatenation of double Holliday junctions during dissolution by Sgs1-Top3. *Nat.*  
582       Struct. Mol. Biol. 17, 1377–1382. <https://doi.org/10.1038/nsmb.1919>
- 583       Cerritelli, S.M., Crouch, R.J., 2009. Ribonuclease H: the enzymes in eukaryotes. *FEBS J.* 276,  
584       1494–1505. <https://doi.org/10.1111/j.1742-4658.2009.06908.x>
- 585       Chakraborty, U., George, C.M., Lyndaker, A.M., Alani, E., 2016. A delicate balance between  
586       repair and replication factors regulates recombination between divergent DNA sequences in  
587       *Saccharomyces cerevisiae*. *Genetics* 202, 525–540.  
588       <https://doi.org/10.1534/genetics.115.184093>
- 589       Chang, M., Bellaoui, M., Zhang, C., Desai, R., Morozov, P., Delgado-Cruzata, L., Rothstein, R.,  
590       Freyer, G.A., Boone, C., Brown, G.W., 2005. *RMII/NCE4*, a suppressor of genome  
591       instability, encodes a member of the RecQ helicase/Topo III complex. *EMBO J.* 24, 2024–

- 592 2033. <https://doi.org/10.1038/sj.emboj.7600684>
- 593 Chavez, S., Beilharz, T., Rondón, A.G., Erdjument-Bromage, H., Tempst, P., Svejstrup, J.Q.,  
594 Lithgow, T., Aguilera, A., 2000. A protein complex containing Tho2, Hpr1, Mft1 and a  
595 novel protein, Thp2, connects transcription elongation with mitotic recombination in  
596 *Saccharomyces cerevisiae*. EMBO J. 19, 5824–5834.  
597 <https://doi.org/10.1093/emboj/19.21.5824>
- 598 Chou, D.M., Elledge, S.J., 2006. Tipin and Timeless form a mutually protective complex  
599 required for genotoxic stress resistance and checkpoint function. Proc. Natl. Acad. Sci. U. S.  
600 A. 103, 18143–18147. <https://doi.org/10.1073/pnas.0609251103>
- 601 Claussin, C., Chang, M., 2015. The many facets of homologous recombination at telomeres.  
602 Microb. Cell 2, 308–321. <https://doi.org/10.15698/mic2015.09.224>
- 603 Claussin, C., Porubský, D., Spierings, D.C.J., Halsema, N., Rentas, S., Guryev, V., Lansdorp,  
604 P.M., Chang, M., 2017. Genome-wide mapping of sister chromatid exchange events in  
605 single yeast cells using strand-seq. Elife 6, e30560. <https://doi.org/10.7554/eLife.30560>
- 606 Clemente-Ruiz, M., Prado, F., 2009. Chromatin assembly controls replication fork stability.  
607 EMBO Rep. 10, 790–796. <https://doi.org/10.1038/embor.2009.67>
- 608 Conover, H.N., Lujan, S.A., Chapman, M.J., Cornelio, D.A., Sharif, R., Williams, J.S., Clark,  
609 A.B., Camilo, F., Kunkel, T.A., Argueso, J.L., 2015. Stimulation of chromosomal  
610 rearrangements by ribonucleotides. Genetics 201, 951–961.  
611 <https://doi.org/10.1534/genetics.115.181149>
- 612 Cornelio, D.A., Sedam, H.N.C., Ferrarezi, J.A., Sampaio, N.M.V., Argueso, J.L., 2017. Both R-  
613 loop removal and ribonucleotide excision repair activities of RNase H2 contribute  
614 substantially to chromosome stability. DNA Repair (Amst). 52, 110–114.  
615 <https://doi.org/10.1016/j.dnarep.2017.02.012>
- 616 Costanzo, M., VanderSluis, B., Koch, E.N., Baryshnikova, A., Pons, C., Tan, G., Wang, W.,  
617 Usaj, M., Hanchard, J., Lee, S.D., Pelechano, V., Styles, E.B., Billmann, M., Van Leeuwen,  
618 J., Van Dyk, N., Lin, Z.Y., Kuzmin, E., Nelson, J., Piotrowski, J.S., Srikumar, T., Bahr, S.,  
619 Chen, Y., Deshpande, R., Kurat, C.F., Li, S.C., Li, Z., Usaj, M.M., Okada, H., Pascoe, N.,  
620 Luis, B.J.S., Sharifpoor, S., Shuteriqi, E., Simpkins, S.W., Snider, J., Suresh, H.G., Tan, Y.,  
621 Zhu, H., Malod-Dognin, N., Janjic, V., Przulj, N., Troyanskaya, O.G., Stagljar, I., Xia, T.,  
622 Ohya, Y., Gingras, A.C., Raught, B., Boutros, M., Steinmetz, L.M., Moore, C.L.,  
623 Rosebrock, A.P., Caudy, A.A., Myers, C.L., Andrews, B., Boone, C., 2016. A global genetic  
624 interaction network maps a wiring diagram of cellular function. Science (80-. ). 353,  
625 aaf1420. <https://doi.org/10.1126/science.aaf1420>
- 626 Crow, Y.J., Leitch, A., Hayward, B.E., Garner, A., Parmar, R., Griffith, E., Ali, M., Semple, C.,  
627 Aicardi, J., Babul-Hirji, R., Baumann, C., Baxter, P., Bertini, E., Chandler, K.E., Chitayat,  
628 D., Cau, D., Déry, C., Fazzi, E., Goizet, C., King, M.D., Klepper, J., Lacombe, D., Lanzi,  
629 G., Lyall, H., Martínez-Frías, M.L., Mathieu, M., McKeown, C., Monier, A., Oade, Y.,  
630 Quarrell, O.W., Rittley, C.D., Rogers, R.C., Sanchis, A., Stephenson, J.B.P., Tacke, U., Till,  
631 M., Tolmie, J.L., Tomlin, P., Voit, T., Weschke, B., Woods, C.G., Lebon, P., Bonthron,

- 632 D.T., Ponting, C.P., Jackson, A.P., 2006. Mutations in genes encoding ribonuclease H2  
633 subunits cause Aicardi-Goutières syndrome and mimic congenital viral brain infection. *Nat.*  
634 *Genet.* 38, 910–916. <https://doi.org/10.1038/ng1842>
- 635 Datta, A., Adjiri, A., New, L., Crouse, G.F., Jinks Robertson, S., 1996. Mitotic crossovers  
636 between diverged sequences are regulated by mismatch repair proteins in *Saccharomyces*  
637 *cerevisiae*. *Mol. Cell. Biol.* 16, 1085–1093. <https://doi.org/10.1128/MCB.16.3.1085>
- 638 de Wind, N., Dekker, M., Berns, A., Radman, M., te Riele, H., 1995. Inactivation of the mouse  
639 Msh2 gene results in mismatch repair deficiency, methylation tolerance,  
640 hyperrecombination, and predisposition to cancer. *Cell* 82, 321–330.  
641 [https://doi.org/10.1016/0092-8674\(95\)90319-4](https://doi.org/10.1016/0092-8674(95)90319-4)
- 642 Delaunay, A., Pflieger, D., Barrault, M.-B., Vinh, J., Toledano, M.B., 2002. A thiol peroxidase is  
643 an H<sub>2</sub>O<sub>2</sub> receptor and redox-transducer in gene activation. *Cell* 111, 471–481.  
644 [https://doi.org/10.1016/S0092-8674\(02\)01048-6](https://doi.org/10.1016/S0092-8674(02)01048-6)
- 645 Dittmar, J.C., Pierce, S., Rothstein, R., Reid, R.J.D., 2013. Physical and genetic-interaction  
646 density reveals functional organization and informs significance cutoffs in genome-wide  
647 screens. *Proc Natl Acad Sci U S A* 110, 7389–7394.  
648 <https://doi.org/10.1073/pnas.1219582110>
- 649 Dittmar, J.C., Reid, R.J.D., Rothstein, R., 2010. ScreenMill: a freely available software suite for  
650 growth measurement, analysis and visualization of high-throughput screen data. *BMC*  
651 *Bioinformatics* 11, 353. <https://doi.org/10.1186/1471-2105-11-353>
- 652 Elliott, B., Jasin, M., 2001. Repair of double-strand breaks by homologous recombination in  
653 mismatch repair-defective mammalian cells. *Mol. Cell. Biol.* 21, 2671–2682.  
654 <https://doi.org/10.1128/MCB.21.8.2671-2682.2001>
- 655 Epshtein, A., Potenski, C., Klein, H., 2016. Increased spontaneous recombination in RNase H2-  
656 deficient cells arises from multiple contiguous rNMPs and not from single rNMP residues  
657 incorporated by DNA polymerase epsilon. *Microb. Cell* 3, 248–254.  
658 <https://doi.org/10.15698/mic2016.06.506>
- 659 Freudenreich, C.H., Su, X.A., 2016. Relocalization of DNA lesions to the nuclear pore complex.  
660 *FEMS Yeast Res.* 16, fow095. <https://doi.org/10.1093/femsyr/fow095>
- 661 George, C.M., Alani, E., 2012. Multiple cellular mechanisms prevent chromosomal  
662 rearrangements involving repetitive DNA. *Crit. Rev. Biochem. Mol. Biol.* 47, 297–313.  
663 <https://doi.org/10.3109/10409238.2012.675644>
- 664 Giaever, G., Chu, A.M., Ni, L., Connelly, C., Riles, L., Véronneau, S., Dow, S., Lucau-Danila,  
665 A., Anderson, K., André, B., Arkin, A.P., Astromoff, A., El Bakkoury, M., Bangham, R.,  
666 Benito, R., Brachat, S., Campanaro, S., Curtiss, M., Davis, K., Deutschbauer, A., Entian,  
667 K.D., Flaherty, P., Foury, F., Garfinkel, D.J., Gerstein, M., Gotte, D., Güldener, U.,  
668 Hegemann, J.H., Hempel, S., Herman, Z., Jaramillo, D.F., Kelly, D.E., Kelly, S.L., Kötter,  
669 P., LaBonte, D., Lamb, D.C., Lan, N., Liang, H., Liao, H., Liu, L., Luo, C., Lussier, M.,  
670 Mao, R., Menard, P., Ooi, S.L., Revuelta, J.L., Roberts, C.J., Rose, M., Ross-Macdonald, P.,

- 671 Scherens, B., Schimmack, G., Shafer, B., Shoemaker, D.D., Sookhai-Mahadeo, S., Storms,  
672 R.K., Strathern, J.N., Valle, G., Voet, M., Volckaert, G., Wang, C. yun, Ward, T.R.,  
673 Wilhelmy, J., Winzeler, E.A., Yang, Y., Yen, G., Youngman, E., Yu, K., Bussey, H., Boeke,  
674 J.D., Snyder, M., Philippsen, P., Davis, R.W., Johnston, M., 2002. Functional profiling of  
675 the *Saccharomyces cerevisiae* genome. *Nature* 418, 387–391.  
676 <https://doi.org/10.1038/nature00935>
- 677 Goldfarb, T., Alani, E., 2005. Distinct roles for the *Saccharomyces cerevisiae* mismatch repair  
678 proteins in heteroduplex rejection, mismatch repair and nonhomologous tail removal.  
679 *Genetics* 169, 563–574. <https://doi.org/10.1534/genetics.104.035204>
- 680 Hendry, J.A., Tan, G., Ou, J., Boone, C., Brown, G.W., 2015. Leveraging DNA damage response  
681 signaling to identify yeast genes controlling genome stability. *G3* 5, 997–1006.  
682 <https://doi.org/10.1534/g3.115.016576>
- 683 Heyer, W.D., 2015. Regulation of recombination and genomic maintenance. *Cold Spring Harb.*  
684 *Perspect. Biol.* 7, a016501. <https://doi.org/10.1101/cshperspect.a016501>
- 685 Hirata, R., Graham, L.A., Takatsuki, A., Stevens, T.H., Anraku, Y., 1997. *VMA11* and *VMA16*  
686 encode second and third proteolipid subunits of the *Saccharomyces cerevisiae* vacuolar  
687 membrane H<sup>+</sup>-ATPase. *J. Biol. Chem.* 272, 4795–4803.  
688 <https://doi.org/10.1074/jbc.272.8.4795>
- 689 Hishida, T., Iwasaki, H., Ohno, T., Morishita, T., Shinagawa, H., 2001. A yeast gene, *MGS1*,  
690 encoding a DNA-dependent AAA<sup>+</sup> ATPase is required to maintain genome stability. *Proc.*  
691 *Natl. Acad. Sci.* 98, 8283–8289. <https://doi.org/10.1073/pnas.121009098>
- 692 Ho, B., Baryshnikova, A., Brown, G.W., 2018. Unification of protein abundance datasets yields a  
693 quantitative *Saccharomyces cerevisiae* proteome. *Cell Syst.* 6, 192–205.  
694 <https://doi.org/10.1016/j.cels.2017.12.004>
- 695 Huang, J., Brito, I.L., Villén, J., Gygi, S.P., Amon, A., Moazed, D., 2006. Inhibition of  
696 homologous recombination by a cohesin-associated clamp complex recruited to the rDNA  
697 recombination enhancer. *Genes Dev.* 20, 2887–2901. <https://doi.org/10.1101/gad.1472706>
- 698 Huang, M.-E., Kolodner, R.D., 2005. A biological network in *Saccharomyces cerevisiae* prevents  
699 the deleterious effects of endogenous oxidative DNA damage. *Mol. Cell* 17, 709–720.  
700 <https://doi.org/10.1016/j.molcel.2005.02.008>
- 701 Huertas, P., Aguilera, A., 2003. Cotranscriptionally formed DNA:RNA hybrids mediate  
702 transcription elongation impairment and transcription-associated recombination. *Mol. Cell*  
703 12, 711–721. <https://doi.org/10.1016/j.molcel.2003.08.010>
- 704 Hughes, A.L., Gottschling, D.E., 2012. An early age increase in vacuolar pH limits mitochondrial  
705 function and lifespan in yeast. *Nature* 492, 261–265. <https://doi.org/10.1038/nature11654>
- 706 Huh, W.-K., Falvo, J. V., Gerke, L.C., Carroll, A.S., Howson, R.W., Weissman, J.S., O’Shea,  
707 E.K., 2003. Global analysis of protein localization in budding yeast. *Nature* 425, 686–691.  
708 <https://doi.org/10.1038/nature02026>

- 709 Hum, Y.F., Jinks-Robertson, S., 2018. DNA strand-exchange patterns associated with double-  
710 strand break-induced and spontaneous mitotic crossovers in *Saccharomyces cerevisiae*.  
711 PLoS Genet. 14, e1007302. <https://doi.org/10.1371/journal.pgen.1007302>
- 712 Hunter, N., 2015. Meiotic recombination: The essence of heredity. Cold Spring Harb. Perspect.  
713 Biol. 7, a016618. <https://doi.org/10.1101/cshperspect.a016618>
- 714 Ivessa, A.S., Lenzmeier, B.A., Bessler, J.B., Goudsouzian, L.K., Schnakenberg, S.L., Zakian,  
715 V.A., 2003. The *Saccharomyces cerevisiae* helicase Rrm3p facilitates replication past  
716 nonhistone protein-DNA complexes. Mol. Cell 12, 1525–1536.  
717 [https://doi.org/10.1016/S1097-2765\(03\)00456-8](https://doi.org/10.1016/S1097-2765(03)00456-8)
- 718 Ivessa, A.S., Zhou, J.Q., Zakian, V.A., 2000. The *Saccharomyces* Pif1p DNA helicase and the  
719 highly related Rrm3p have opposite effects on replication fork progression in ribosomal  
720 DNA. Cell 100, 479–489. [https://doi.org/10.1016/S0092-8674\(00\)80683-2](https://doi.org/10.1016/S0092-8674(00)80683-2)
- 721 Johnson, R.D., Jasin, M., 2000. Sister chromatid gene conversion is a prominent double-strand  
722 break repair pathway in mammalian cells. EMBO J. 19, 3398–3407.  
723 <https://doi.org/10.1093/emboj/19.13.3398>
- 724 Kadyk, L.C., Hartwell, L.H., 1992. Sister chromatids are preferred over homologs as substrates  
725 for recombinational repair in *Saccharomyces cerevisiae*. Genetics 132, 387–402.  
726 <https://doi.org/10.1128/EC.3.6.1492>
- 727 Kane, P.M., 2006. The where, when, and how of organelle acidification by the yeast vacuolar  
728 H<sup>+</sup>-ATPase. Microbiol. Mol. Biol. Rev. 70, 177–191.  
729 <https://doi.org/10.1128/MMBR.70.1.177>
- 730 Katou, Y., Kanoh, Y., Bando, M., Noguchi, H., Tanaka, H., Ashikari, T., Sugimoto, K.,  
731 Shirahige, K., 2003. S-phase checkpoint proteins Tof1 and Mrc1 form a stable replication-  
732 pausing complex. Nature 424, 1078–1083. <https://doi.org/10.1038/nature01900>
- 733 Keil, R.L., McWilliams, A.D., 1993. A gene with specific and global effects on recombination of  
734 sequences from tandemly repeated genes in *Saccharomyces cerevisiae*. Genetics 135, 711–  
735 718. [https://doi.org/10.1016/0168-9525\(94\)90142-2](https://doi.org/10.1016/0168-9525(94)90142-2)
- 736 Kerscher, O., Hieter, P., Winey, M., Basrai, M.A., 2001. Novel role for a *Saccharomyces*  
737 *cerevisiae* nucleoporin, Nup170p, in chromosome segregation. Genetics 157, 1543–1553.
- 738 Keskin, H., Shen, Y., Huang, F., Patel, M., Yang, T., Ashley, K., Mazin, A. V., Storici, F., 2014.  
739 Transcript-RNA-templated DNA recombination and repair. Nature 515, 436–439.  
740 <https://doi.org/10.1038/nature13682>
- 741 Krejci, L., Altmannova, V., Spirek, M., Zhao, X., 2012. Homologous recombination and its  
742 regulation. Nucleic Acids Res. 40, 5795–5818. <https://doi.org/10.1093/nar/gks270>
- 743 Kuzmin, E., Costanzo, M., Andrews, B., Boone, C., 2016. Synthetic genetic array analysis. Cold  
744 Spring Harb. Protoc. 2016, pdb.prot088807. <https://doi.org/10.1101/pdb.prot088807>
- 745 Lea, D.E., Coulson, C.A., 1949. The distribution of the numbers of mutants in bacterial

- 746 populations. *J. Genet.* 49, 264–285.
- 747 Lehner, K.R., Stone, M.M., Farber, R.A., Petes, T.D., 2007. Ninety-six haploid yeast strains with  
748 individual disruptions of Open Reading Frames between *YOR097C* and *YOR192C*,  
749 constructed for the *Saccharomyces* Genome Deletion Project, have an additional mutation in  
750 the Mismatch Repair gene *MSH3*. *Genetics* 177, 1951–1953.  
751 <https://doi.org/10.1534/genetics.107.079368>
- 752 Leman, A.R., Noguchi, C., Lee, C.Y., Noguchi, E., 2010. Human Timeless and Tipin stabilize  
753 replication forks and facilitate sister-chromatid cohesion. *J. Cell Sci.*  
754 <https://doi.org/10.1242/jcs.057984>
- 755 Leuzzi, G., Marabitti, V., Pichierri, P., Franchitto, A., 2016. WRNIP1 protects stalled forks from  
756 degradation and promotes fork restart after replication stress. *EMBO J.* 35, 1437–1451.  
757 <https://doi.org/10.15252/embj.201593265>
- 758 Liang, D., Burkhart, S.L., Singh, R.K., Kabbaj, M.H.M., Gunjan, A., 2012. Histone dosage  
759 regulates DNA damage sensitivity in a checkpoint-independent manner by the homologous  
760 recombination pathway. *Nucleic Acids Res.* 40, 9604–9620.  
761 <https://doi.org/10.1093/nar/gks722>
- 762 López-Flores, I., Garrido-Ramos, M.A., 2012. The repetitive DNA content of eukaryotic  
763 genomes. *Genome Dyn.* 7, 1–28. <https://doi.org/10.1159/000337118>
- 764 Luria, S.E., Delbrück, M., 1943. Mutations of bacteria from virus sensitivity to virus resistance.  
765 *Genetics* 28, 491–511.
- 766 Mayer, M.L., Pot, I., Chang, M., Xu, H., Aneliunas, V., Kwok, T., Newitt, R., Aebersold, R.,  
767 Boone, C., Brown, G.W., Hieter, P., 2004. Identification of protein complexes required for  
768 efficient sister chromatid cohesion. *Mol. Biol. Cell* 15, 1736–1745.  
769 <https://doi.org/10.1091/mbc.E03-08-0619>
- 770 McVey, M., Khodaverdian, V.Y., Meyer, D., Cerqueira, P.G., Heyer, W.-D., 2016. Eukaryotic  
771 DNA polymerases in homologous recombination. *Annu. Rev. Genet.* 50, 393–421.  
772 <https://doi.org/10.1146/annurev-genet-120215-035243>
- 773 Mekhail, K., Seebacher, J., Gygi, S.P., Moazed, D., 2008. Role for perinuclear chromosome  
774 tethering in maintenance of genome stability. *Nature* 456, 667–670.  
775 <https://doi.org/10.1038/nature07460>
- 776 Milgrom, E., Diab, H., Middleton, F., Kane, P.M., 2007. Loss of vacuolar proton-translocating  
777 ATPase activity in yeast results in chronic oxidative stress. *J. Biol. Chem.* 282, 7125–7136.  
778 <https://doi.org/10.1074/jbc.M608293200>
- 779 Mohanty, B.K., Bairwa, N.K., Bastia, D., 2006. The Tof1p-Csm3p protein complex counteracts  
780 the Rrm3p helicase to control replication termination of *Saccharomyces cerevisiae*. *Proc.*  
781 *Natl. Acad. Sci. U. S. A.* 103, 897–902. <https://doi.org/10.1073/pnas.0506540103>
- 782 Morano, K.A., Grant, C.M., Moye-Rowley, W.S., 2012. The response to heat shock and  
783 oxidative stress in *Saccharomyces cerevisiae*. *Genetics* 190, 1157–1195.

- 784 <https://doi.org/10.1534/genetics.111.128033>
- 785 Myung, K., Datta, A., Chen, C., Kolodner, R.D., 2001. *SGS1*, the *Saccharomyces cerevisiae*  
786 homologue of BLM and WRN, suppresses genome instability and homeologous  
787 recombination. *Nat. Genet.* 27, 113–116. <https://doi.org/10.1038/83673>
- 788 Nicholson, A., Hendrix, M., Jinks-Robertson, S., Crouse, G.F., 2000. Regulation of mitotic  
789 homeologous recombination in yeast: functions of mismatch repair and nucleotide excision  
790 repair genes. *Genetics* 154, 133–146.
- 791 Noguchi, E., Noguchi, C., Du, L.-L., Russell, P., 2003. Swi1 prevents replication fork collapse  
792 and controls checkpoint kinase Cds1. *Mol. Cell. Biol.* 23, 7861–7874.  
793 <https://doi.org/10.1128/MCB.23.21.7861-7874.2003>
- 794 Noguchi, E., Noguchi, C., McDonald, W.H., Yates, J.R., Russell, P., 2004. Swi1 and Swi3 are  
795 components of a Replication Fork Protection Complex in fission yeast. *Mol. Cell. Biol.* 24,  
796 8342–8355. <https://doi.org/10.1128/MCB.24.19.8342-8355.2004>
- 797 Novarina, D., Janssens, G.E., Bokern, K., Schut, T., van Oerle, N.C., Kazemier, H.G., Veenhoff,  
798 L.M., Chang, M., 2020. A genome-wide screen identifies genes that suppress the  
799 accumulation of spontaneous mutations in young and aged yeast cells. *Aging Cell* 19,  
800 e13084. <https://doi.org/10.1111/ace1.13084>
- 801 O’Connell, K., Jinks-Robertson, S., Petes, T.D., 2015. Elevated Genome-wide instability in yeast  
802 mutants lacking RNase H activity. *Genetics* 201, 963–975.  
803 <https://doi.org/10.1534/genetics.115.182725>
- 804 Owiti, N., Lopez, C., Singh, S., Stephenson, A., Kim, N., 2017. Def1 and Dst1 play distinct roles  
805 in repair of AP lesions in highly transcribed genomic regions. *DNA Repair (Amst.)* 55, 31–  
806 39. <https://doi.org/10.1016/j.dnarep.2017.05.003>
- 807 Pan, X., Ye, P., Yuan, D.S., Wang, X., Bader, J.S., Boeke, J.D., 2006. A DNA integrity network  
808 in the yeast *Saccharomyces cerevisiae*. *Cell* 124, 1069–1081.  
809 <https://doi.org/10.1016/j.cell.2005.12.036>
- 810 Poon, B.P.K., Mekhail, K., 2011. Cohesin and related coiled-coil domain-containing complexes  
811 physically and functionally connect the dots across the genome. *Cell Cycle* 10, 2669–2682.  
812 <https://doi.org/10.4161/cc.10.16.17113>
- 813 Popoff, S.C., Spira, A.I., Johnson, A.W., Demple, B., 1990. Yeast structural gene (*APNI*) for the  
814 major apurinic endonuclease: homology to *Escherichia coli* endonuclease IV. *Proc. Natl.*  
815 *Acad. Sci. U. S. A.* 87, 4193–4197. <https://doi.org/10.1073/pnas.87.11.4193>
- 816 Potenski, C.J., Niu, H., Sung, P., Klein, H.L., 2014. Avoidance of ribonucleotide-induced  
817 mutations by RNase H2 and Srs2-Exo1 mechanisms. *Nature* 511, 251–254.  
818 <https://doi.org/10.1038/nature13292>
- 819 Prado, F., Aguilera, A., 2005. Partial depletion of histone H4 increases homologous  
820 recombination-mediated genetic instability. *Mol. Cell. Biol.* 25, 1526–1536.  
821 <https://doi.org/10.1128/mcb.25.4.1526-1536.2005>

- 822 Prakash, S., Prakash, L., 2000. Nucleotide excision repair in yeast. *Mutat. Res.* 451, 13–24.  
823 [https://doi.org/10.1016/S0027-5107\(00\)00037-3](https://doi.org/10.1016/S0027-5107(00)00037-3)
- 824 Saugar, I., Parker, J.L., Zhao, S., Ulrich, H.D., 2012. The genome maintenance factor Mgs1 is  
825 targeted to sites of replication stress by ubiquitylated PCNA. *Nucleic Acids Res.* 40, 245–  
826 257. <https://doi.org/10.1093/nar/gkr738>
- 827 Schalbetter, S.A., Mansoubi, S., Chambers, A.L., Downs, J.A., Baxter, J., 2015. Fork rotation and  
828 DNA precatenation are restricted during DNA replication to prevent chromosomal  
829 instability. *Proc. Natl. Acad. Sci.* 112, E4565–E4570.  
830 <https://doi.org/10.1073/pnas.1505356112>
- 831 Schmidt, K.H., Kolodner, R.D., 2004. Requirement of Rrm3 helicase for repair of spontaneous  
832 DNA lesions in cells lacking Srs2 or Sgs1 helicase. *Mol. Cell. Biol.* 24, 3213–3226.  
833 <https://doi.org/10.1128/MCB.24.8.3213>
- 834 Schneider, C.A., Rasband, W.S., Eliceiri, K.W., 2012. NIH Image to ImageJ : 25 years of image  
835 analysis. *Nat. Methods* 9, 671–675. <https://doi.org/10.1038/nmeth.2089>
- 836 Sherman, F., 2002. Getting started with yeast. *Methods Enzymol.* 350, 3–41.  
837 [https://doi.org/http://dx.doi.org/10.1016/S0076-6879\(02\)50954-X](https://doi.org/http://dx.doi.org/10.1016/S0076-6879(02)50954-X)
- 838 Smith, J., Rothstein, R., 1999. An allele of *RFA1* suppresses *RAD52*-dependent double-strand  
839 break repair in *Saccharomyces cerevisiae*. *Genetics* 151, 447–458.
- 840 Sommariva, E., Pellny, T.K., Karahan, N., Kumar, S., Huberman, J.A., Dalgaard, J.Z., 2005.  
841 *Schizosaccharomyces pombe* Swi1, Swi3, and Hsk1 are components of a novel S-phase  
842 response pathway to alkylation damage. *Mol. Cell. Biol.* 25, 2770–2784.  
843 <https://doi.org/10.1128/MCB.25.7.2770-2784.2005>
- 844 Spell, R.M., Jinks-Robertson, S., 2004. Examination of the roles of Sgs1 and Srs2 helicases in the  
845 enforcement of recombination fidelity in *Saccharomyces cerevisiae*. *Genetics* 168, 1855–  
846 1865. <https://doi.org/10.1534/genetics.104.032771>
- 847 Spies, M., Fishel, R., 2015. Mismatch repair during homologous and homeologous  
848 recombination. *Cold Spring Harb. Perspect. Biol.* 7, a022657.  
849 <https://doi.org/10.1101/cshperspect.a022657>
- 850 Stirling, P.C., Bloom, M.S., Solanki-Patil, T., Smith, S., Sipahimalani, P., Li, Z., Kofoed, M.,  
851 Ben-Aroya, S., Myung, K., Hieter, P., 2011. The complete spectrum of yeast chromosome  
852 instability genes identifies candidate CIN cancer genes and functional roles for ASTRA  
853 complex components. *PLoS Genet.* 7, e1002057.  
854 <https://doi.org/10.1371/journal.pgen.1002057>
- 855 Styles, E.B., Founk, K.J., Zamparo, L.A., Sing, T.L., Altintas, D., Ribeyre, C., Ribaud, V.,  
856 Rougemont, J., Mayhew, D., Costanzo, M., Usaj, M., Verster, A.J., Koch, E.N., Novarina,  
857 D., Graf, M., Luke, B., Muzi-Falconi, M., Myers, C.L., Mitra, R.D., Shore, D., Brown,  
858 G.W., Zhang, Z., Boone, C., Andrews, B.J., 2016. Exploring quantitative yeast phenomics  
859 with single-cell analysis of DNA damage foci. *Cell Syst.* 3, 264–277.e10.



- 860 Sugawara, N., Goldfarb, T., Studamire, B., Alani, E., Haber, J.E., 2004. Heteroduplex rejection  
861 during single-strand annealing requires Sgs1 helicase and mismatch repair proteins Msh2  
862 and Msh6 but not Pms1. *Proc. Natl. Acad. Sci. U. S. A.* 101, 9315–9320.  
863 <https://doi.org/10.1073/pnas.0305749101>
- 864 Supek, F., Bošnjak, M., Škunca, N., Šmuc, T., 2011. REVIGO summarizes and visualizes long  
865 lists of Gene Ontology terms. *PLoS One* 6, e21800.  
866 <https://doi.org/10.1371/journal.pone.0021800>
- 867 Swanson, R.L., Morey, N.J., Doetsch, P.W., Jinks-Robertson, S., 1999. Overlapping specificities  
868 of base excision repair, nucleotide excision repair, recombination, and translesion synthesis  
869 pathways for DNA base damage in *Saccharomyces cerevisiae*. *Mol. Cell. Biol.* 19, 2929–  
870 2935. <https://doi.org/10.1128/MCB.19.4.2929>
- 871 Symington, L.S., Rothstein, R., Lisby, M., 2014. Mechanisms and regulation of mitotic  
872 recombination in *Saccharomyces cerevisiae*. *Genetics* 198, 795–835.  
873 <https://doi.org/10.1534/genetics.114.166140>
- 874 Thorpe, G.W., Fong, C.S., Alic, N., Higgins, V.J., Dawes, I.W., 2004. Cells have distinct  
875 mechanisms to maintain protection against different reactive oxygen species: Oxidative-  
876 stress-response genes. *Proc. Natl. Acad. Sci.* 101, 6564–6569.  
877 <https://doi.org/10.1073/pnas.0305888101>
- 878 Torres, J.Z., Schnakenberg, S.L., Zakian, V.A., 2004. *Saccharomyces cerevisiae* Rrm3p DNA  
879 helicase promotes genome integrity by preventing replication fork stalling: viability of *rrm3*  
880 cells requires the intra-S-phase checkpoint and fork restart activities. *Mol. Cell. Biol.* 24,  
881 3198–3212. <https://doi.org/10.1128/MCB.24.8.3198-3212.2004>
- 882 Treco, D.A., Lundblad, V., 2001. Preparation of yeast media. *Curr. Protoc. Mol. Biol.* Chapter  
883 13, Unit13.1. <https://doi.org/10.1002/0471142727.mb1301s23>
- 884 Tsurimoto, T., Shinozaki, A., Yano, M., Seki, M., Enomoto, T., 2005. Human Werner helicase  
885 interacting protein 1 (WRNIP1) functions as novel modulator for DNA polymerase  $\delta$ .  
886 *Genes to Cells* 10, 13–22. <https://doi.org/10.1111/j.1365-2443.2004.00812.x>
- 887 Ulrich, H.D., 2005. The *RAD6* pathway: Control of DNA damage bypass and mutagenesis by  
888 ubiquitin and SUMO. *ChemBioChem* 6, 1735–1743.  
889 <https://doi.org/10.1002/cbic.200500139>
- 890 Umemoto, N., Ohya, Y., Anraku, Y., 1991. *VMA11*, a novel gene that encodes a putative  
891 proteolipid, is indispensable for expression of yeast vacuolar membrane  $H^+$ -ATPase activity.  
892 *J. Biol. Chem.* 266, 24526–24532.
- 893 Urtishak, K.A., Smith, K.D., Chanoux, R.A., Greenberg, R.A., Johnson, F.B., Brown, E.J., 2009.  
894 Timeless maintains genomic stability and suppresses sister chromatid exchange during  
895 unperturbed DNA replication. *J. Biol. Chem.* 284, 8777–8785.  
896 <https://doi.org/10.1074/jbc.M806103200>
- 897 Usaj, M., Tan, Y., Wang, W., VanderSluis, B., Zou, A., Myers, C.L., Costanzo, M., Andrews, B.,  
898 Boone, C., 2017. TheCellMap.org: a web-accessible database for visualizing and mining the

- 899 global yeast genetic interaction network. *G3* (Bethesda). 7, 1539–1549.  
900 <https://doi.org/10.1534/g3.117.040220>
- 901 Vance, J.R., Wilson, T.E., 2001. Repair of DNA strand breaks by the overlapping functions of  
902 lesion-specific and non-lesion-specific DNA 3' phosphatases. *Mol. Cell. Biol.* 21, 7191–  
903 7198. <https://doi.org/10.1128/MCB.21.21.7191-7198.2001>
- 904 Veatch, J.R., McMurray, M.A., Nelson, Z.W., Gottschling, D.E., 2009. Mitochondrial  
905 dysfunction leads to nuclear genome instability via an iron-sulphur cluster defect. *Cell* 137,  
906 1247–1258. <https://doi.org/10.1016/j.cell.2009.04.014>
- 907 Warde-Farley, D., Donaldson, S.L., Comes, O., Zuberi, K., Badrawi, R., Chao, P., Franz, M.,  
908 Grouios, C., Kazi, F., Lopes, C.T., Maitland, A., Mostafavi, S., Montojo, J., Shao, Q.,  
909 Wright, G., Bader, G.D., Morris, Q., 2010. The GeneMANIA prediction server: biological  
910 network integration for gene prioritization and predicting gene function. *Nucleic Acids Res.*  
911 38, W214–220. <https://doi.org/10.1093/nar/gkq537>
- 912 Wong, C.M., Siu, K.L., Jin, D.Y., 2004. Peroxiredoxin-null yeast cells are hypersensitive to  
913 oxidative stress and are genomically unstable. *J. Biol. Chem.* 279, 23207–23213.  
914 <https://doi.org/10.1074/jbc.M402095200>
- 915 Wu, L., Bachrati, C.Z., Ou, J., Xu, C., Yin, J., Chang, M., Wang, W., Li, L., Brown, G.W.,  
916 Hickson, I.D., 2006. BLAP75/RMI1 promotes the BLM-dependent dissolution of  
917 homologous recombination intermediates. *Proc. Natl. Acad. Sci.* 103, 4068–4073.  
918 <https://doi.org/10.1073/pnas.0508295103>
- 919 Xia, L., Jaafar, L., Cashikar, A., Flores-Rozas, H., 2007. Identification of genes required for  
920 protection from doxorubicin by a genome-wide screen in *Saccharomyces cerevisiae*. *Cancer*  
921 *Res.* 67, 11411–11418. <https://doi.org/10.1158/0008-5472.CAN-07-2399>
- 922 Xiao, W., Samson, L., 1993. In vivo evidence for endogenous DNA alkylation damage as a  
923 source of spontaneous mutation in eukaryotic cells. *Proc. Natl. Acad. Sci. U. S. A.* 90,  
924 2117–2121. <https://doi.org/10.1073/pnas.90.6.2117>
- 925 Xu, H., Boone, C., Klein, H.L., 2004. Mrc1 is required for sister chromatid cohesion to aid in  
926 recombination repair of spontaneous damage. *Mol. Cell. Biol.* 24, 7082–7090.  
927 <https://doi.org/10.1128/MCB.24.16.7082-7090.2004>
- 928 Yang, J., Bachrati, C.Z., Ou, J., Hickson, I.D., Brown, G.W., 2010. Human topoisomerase III $\alpha$  is  
929 a single-stranded DNA decatenase that is stimulated by BLM and RMI1. *J. Biol. Chem.* 285,  
930 21426–21436. <https://doi.org/10.1074/jbc.M110.123216>
- 931 Yi, D.G., Kim, M.J., Choi, J.E., Lee, J., Jung, J., Huh, W.K., Chung, W.H., 2016. Yap1 and Skn7  
932 genetically interact with Rad51 in response to oxidative stress and DNA double-strand break  
933 in *Saccharomyces cerevisiae*. *Free Radic. Biol. Med.* 101, 424–433.  
934 <https://doi.org/10.1016/j.freeradbiomed.2016.11.005>
- 935 Zhang, C., 2014. Essential functions of iron-requiring proteins in DNA replication, repair and cell  
936 cycle control. *Protein Cell* 5, 750–760. <https://doi.org/10.1007/s13238-014-0083-7>



938 FIGURE LEGENDS

939

940 **Figure 1. A genome-wide patching and replica plating screen for mutants with increased**  
941 **direct-repeat recombination.**

942 (A) The *leu2* direct-repeat recombination assay. Spontaneous recombination between two *leu2*  
943 heteroalleles, either through gene conversion or intra-chromosomal single strand annealing  
944 (SSA), yields a functional *LEU2* gene. (B) Schematic representation of the screen based on  
945 patching and replica plating. The *leu2* direct-repeat recombination cassette was introduced into  
946 the yeast deletion collection (YKO) by crossing the collection with a query strain containing the  
947 cassette. Haploid strains containing each gene deletion and the recombination cassette were  
948 isolated using SGA methodology. Each strain was patched on rich medium and replica-plated to  
949 selective medium, where hyper-recombinant mutants form papillae on the surface of the patch.  
950 Recombination rates were measured for positives from the patch assay using fluctuation tests. (C)  
951 Example plates from the patch assay. Each plate bears a negative control (wild type) and a  
952 positive control (*elg1Δ*). Two positive hits from the screen (*rad4Δ*, *ydl162cΔ*) are shown. (D)  
953 Recombination rates are plotted for the validated positives from the patch screen, alongside the  
954 wild-type strain. Each data point is from an independent fluctuation test, with  $n \geq 3$  for each strain.  
955 The vertical bars indicate the mean recombination rate for each strain. (E) The top 10 statistically  
956 supported GO terms enriched in the hits from the patch assay screen are shown, with the -fold  
957 enrichment for each term.

958

959 **Figure 2. A high-throughput replica-pinning screen for genes controlling direct-repeat**  
960 **recombination.**

961 (A) Schematic representation of the screen based on high-throughput replica-pinning. The *leu2*  
962 direct-repeat recombination cassette was introduced into the yeast deletion collection as in Figure  
963 1B. The resulting strains were amplified by parallel high-throughput replica pinning and  
964 subsequently replica-pinned to media lacking leucine to select for recombination events.  
965 Recombination frequencies were calculated for each strain of the YKO collection. (B)  
966 Recombination frequency distribution for the YKO collection (*MSH3* strains) and for the *msh3*  
967 strains in the collection. Recombination frequencies for a wild-type and for a recombination-  
968 defective *rad54* $\Delta$  strain derived from a pilot experiment are indicated by the dashed lines. (C)  
969 Interaction densities determined by CLIK analysis are plotted as a two-dimensional heatmap. The  
970 cutoffs established by CLIK analysis for hyper-recombination (hyper-rec) and recombination-  
971 defective (hypo-rec) genes are shown in the insets. (D) The statistically supported GO terms  
972 enriched in the hits from the pinning assay screen are shown, with the enrichment for each term.  
973 (E) Recombination rates from fluctuation tests of *csml1* $\Delta$  and *nup170* $\Delta$  are plotted. Each data  
974 point is from an independent fluctuation test, with n=3 for each strain. The vertical bars indicate  
975 the mean recombination rate for each strain and the wild-type data from Figure 1D are plotted for  
976 comparison.

977

### 978 **Figure 3. Functional analysis of validated hyper-rec genes.**

979 (A) The overlap of the hyper-rec genes for the two screens is plotted as a Venn diagram. The 15  
980 genes identified in both screens are indicated. (B) A protein-protein interaction network for the  
981 proteins encoded by the 35 validated hyper-rec genes is shown. Nodes represent the proteins, and  
982 are colored to indicate function. Edges indicate a physical interaction as annotated in the  
983 GeneMania database. (C) Spatial analysis of functional enrichment. On the left, the yeast genetic  
984 interaction similarity network is annotated with GO biological process terms to identify major

985 functional domains (Costanzo et al. 2016). 11 of the 17 domains are labeled and delineated by  
986 coloured outlines. On the right, the network is annotated with the 35 validated hyper-rec genes.  
987 The overlay indicates the functional domains annotated on the left. Only nodes with statistically  
988 supported enrichments (SAFE score  $> 0.08$ ,  $p < 0.05$ ) are coloured. **(D)** The 35 validated hyper-  
989 rec genes are compared with existing *Saccharomyces* Genome Database annotations and genome  
990 instability datasets that measured Rad52 focus formation (Alvaro et al., 2007; Styles et al., 2016),  
991 *RNR3* induction (Hendry et al., 2015), or chromosome instability (CIN; (Stirling et al., 2011)). A  
992 green bar indicates that the gene has the given annotation or was detected in the indicated screen.  
993

994 **Figure 4. Spatial analysis of functional enrichment for four hyper-rec genes.** The genetic  
995 interactions of each of the indicated genes was tested for enrichments in the functional  
996 neighbourhoods of the yeast genetic interaction similarity network. The overlay indicates a subset  
997 of functional domains as annotated on Figure 3C. Nodes with statistically supported enrichments  
998 (Neighbourhood enrichment  $p < 0.05$ ) are coloured, black for negative genetic interactions and  
999 red for positive genetic interactions.

1000

1001

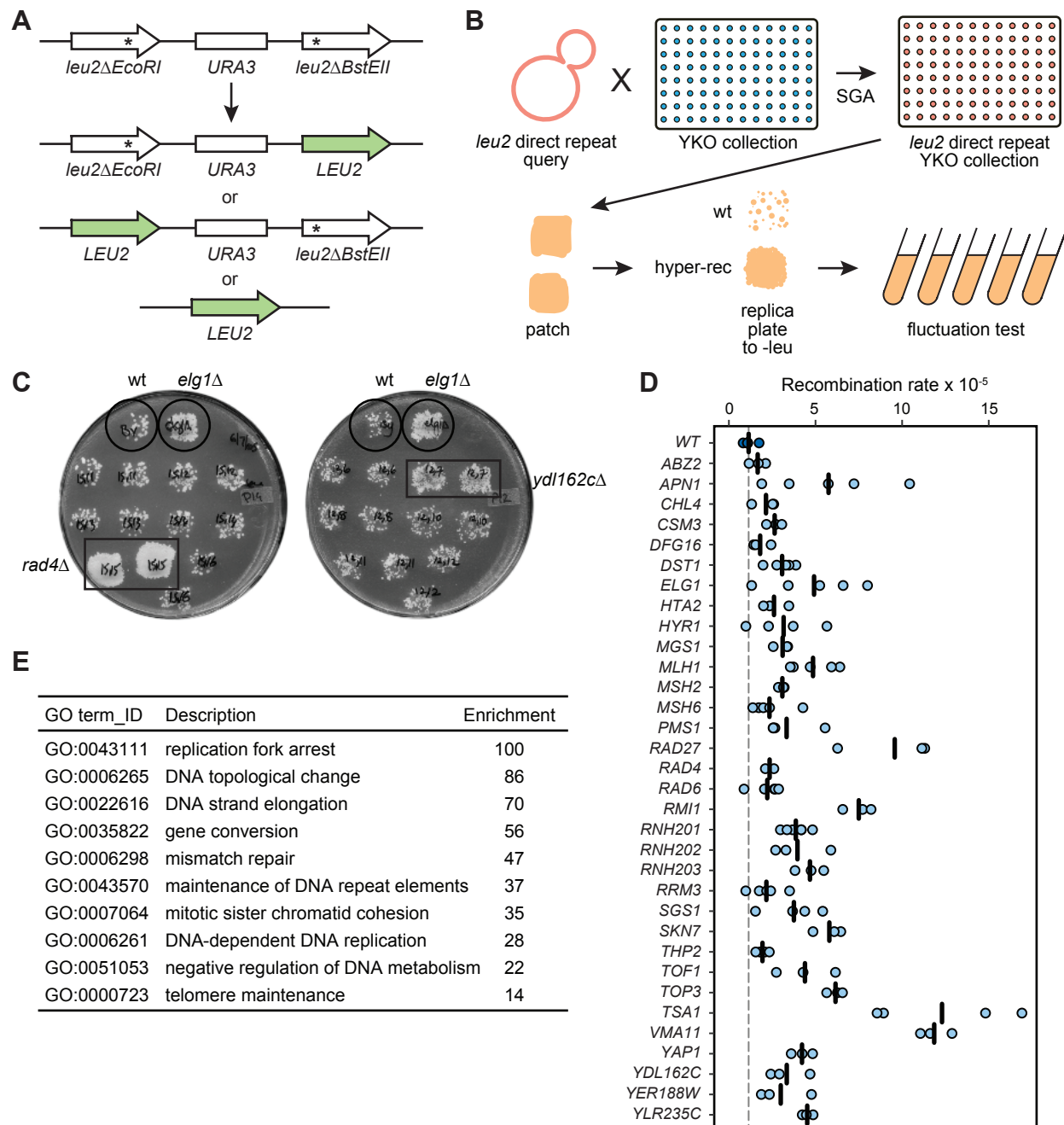


**Figure 1. A genome-wide patching and replica plating screen for mutants with increased direct-repeat recombination. (A)** The *leu2* direct-repeat recombination assay. Spontaneous recombination between two *leu2* heteroalleles, either through gene conversion or intra-chromosomal single strand annealing (SSA), yields a functional *LEU2* gene. **(B)** Schematic representation of the screen based on patching and replica plating. The *leu2* direct-repeat recombination cassette was introduced into the yeast deletion collection (YKO) by crossing the collection with a query strain containing the cassette. Haploid strains containing each gene deletion and the recombination cassette were isolated using SGA methodology. Each strain was patched on rich medium and replica-plated to selective medium, where hyper-recombinant mutants form papillae on the surface of the patch. Recombination rates were measured for positives from the patch assay using fluctuation tests. **(C)** Example plates from the patch assay. Each plate bears a negative control (wild type) and a positive control (*elg1Δ*). Two positive hits from the screen (*rad4Δ*, *ydl162cΔ*) are shown. **(D)** Recombination rates are plotted for the validated positives from the patch screen, alongside the wild-type strain. Each data point is from an independent fluctuation test, with  $n \geq 3$  for each strain. The vertical bars indicate the mean recombination rate for each strain. **(E)** The top 10 statistically supported GO terms enriched in the hits from the patch assay screen are shown, with the -fold enrichment for each term.

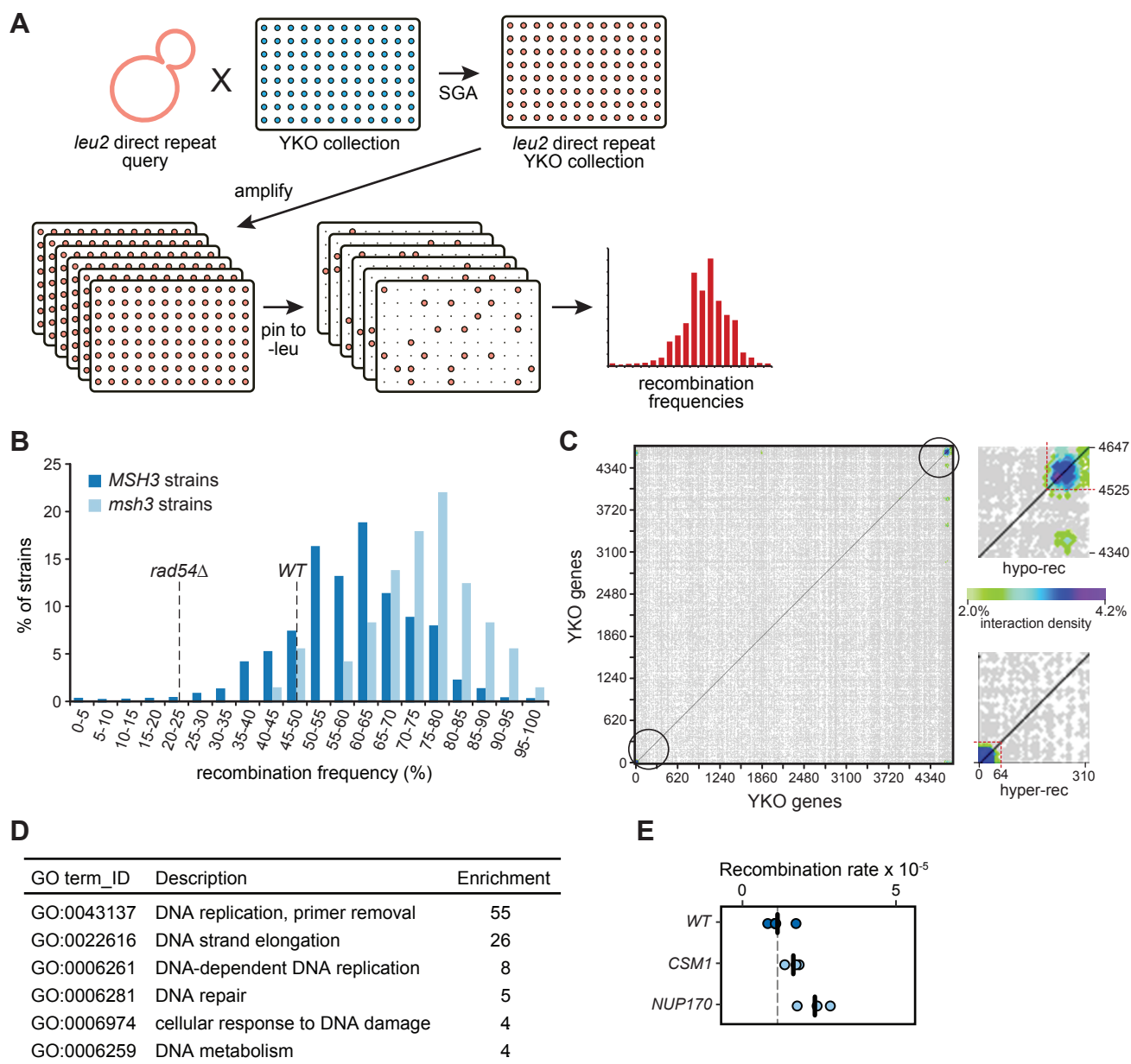


**Figure 2. A high-throughput replica-pinning screen for genes controlling direct-repeat recombination. (A)** Schematic representation of the screen based on high-throughput replica-pinning. The *leu2* direct-repeat recombination cassette was introduced into the yeast deletion collection as in Figure 1B. The resulting strains were amplified by parallel high-throughput replica pinning and subsequently replica-pinned to media lacking leucine to select for recombination events. Recombination frequencies were calculated for each strain of the YKO collection. **(B)** Recombination frequency distribution for the YKO collection (*MSH3* strains) and for the *msh3* strains in the collection. Recombination frequencies for a wild-type and for a recombination-defective *rad54* $\Delta$  strain derived from a pilot experiment are indicated by the dashed lines. **(C)** Interaction densities determined by CLIK analysis are plotted as a two-dimensional heatmap. The cutoffs established by CLIK analysis for hyper-recombination (hyper-rec) and recombination-defective (hypo-rec) genes are shown in the insets. **(D)** The statistically supported GO terms enriched in the hits from the pinning assay screen are shown, with the enrichment for each term. **(E)** Recombination rates from fluctuation tests of *csm1* $\Delta$  and *nup170* $\Delta$  are plotted. Each data point is from an independent fluctuation test, with  $n=3$  for each strain. The vertical bars indicate the mean recombination rate for each strain and the wild-type data from Figure 1D are plotted for comparison.



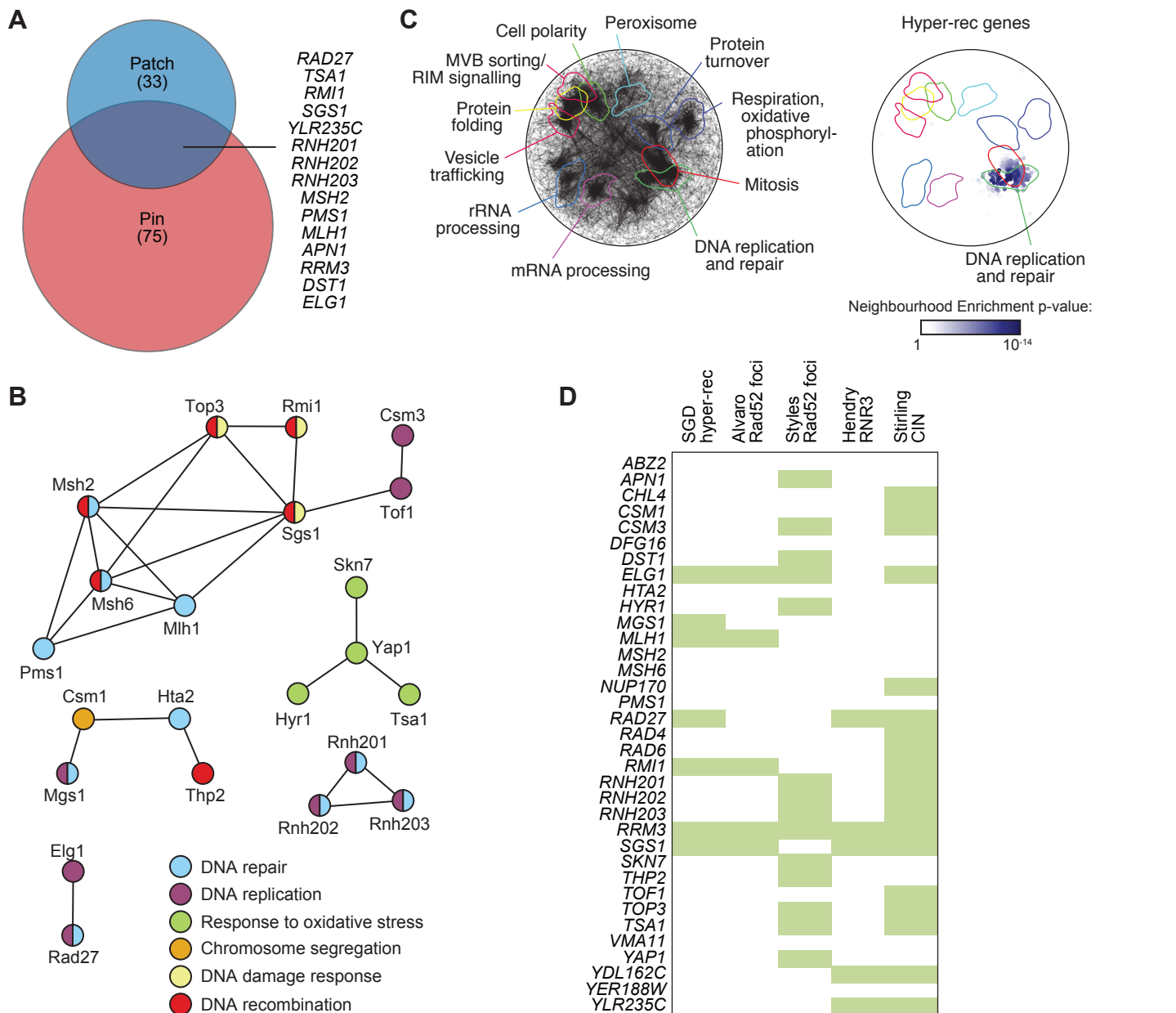


**Figure 3. Functional analysis of validated hyper-rec genes. (A)** The overlap of the hyper-rec genes for the two screens is plotted as a Venn diagram. The 15 genes identified in both screens are indicated. **(B)** A protein-protein interaction network for the proteins encoded by the 35 validated hyper-rec genes is shown. Nodes represent the proteins, and are colored to indicate function. Edges indicate a physical interaction as annotated in the GeneMania database. **(C)** Spatial analysis of functional enrichment. On the left, the yeast genetic interaction similarity network is annotated with GO biological process terms to identify major functional domains (Costanzo et al., 2016). 11 of the 17 domains are labeled and delineated by coloured outlines. On the right, the network is annotated with the 35 validated hyper-rec genes. The overlay indicates the functional domains annotated on the left. Only nodes with statistically supported enrichments (SAFE score > 0.08,  $p < 0.05$ ) are coloured. **(D)** The 35 validated hyper-rec genes are compared with existing Saccharomyces Genome Database annotations and genome instability datasets that measured Rad52 focus formation (Alvaro et al., 2007; Styles et al., 2016), RNR3 induction (Hendry et al., 2015), or chromosome instability (CIN; (Stirling et al., 2011)). A green bar indicates that the gene has the given annotation or was detected in the indicated screen.

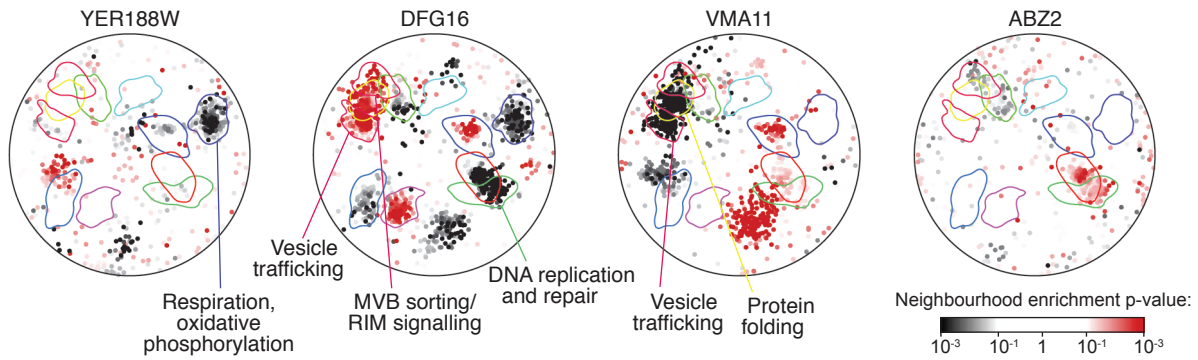


**Figure 4. Spatial analysis of functional enrichment for four hyper-rec genes.** The genetic interactions of each of the indicated genes was tested for enrichments in the functional neighbourhoods of the yeast genetic interaction similarity network. The overlay indicates a subset of functional domains as annotated on Figure 3C. Nodes with statistically supported enrichments (Neighbourhood enrichment  $p < 0.05$ ) are coloured, black for negative genetic interactions and red for positive genetic interactions.

**Table 1. Hyper-recombination genes from the patch assay and pinning assay screens.**

Patch Assay				Pinning Assay Hyper-Rec			
Gene name	Mean recombination rate <sup>a</sup>	Standard deviation	p-value <sup>b</sup>	Gene name	Recombinant colonies (%)	Gene name	Recombinant colonies (%)
WT	1.14E-05	2.84E-06		<i>CSM1</i>	100	<i>RNH201</i>	90
<i>TSA1</i>	1.23E-04	3.64E-05	7.76E-05	<i>ELG1</i>	100	<i>YGL159W</i>	90
<i>VMA11</i>	1.19E-04	7.62E-06	1.27E-08	<i>MSH2</i>	100	<i>YJL043W</i>	90
<i>RAD27</i>	9.39E-05	2.59E-05	1.26E-04	<i>RAD27</i>	100	<i>YLR279W</i>	90
<i>RMI1</i>	7.50E-05	6.85E-06	2.65E-07	<i>RRM3</i>	100	<i>YOR082C</i>	90
<i>TOP3</i>	6.15E-05	3.80E-06	1.13E-07	<i>SGS1</i>	100	<i>ARP8</i>	88
<i>SKN7</i>	5.80E-05	6.85E-06	2.20E-06	<i>TSA1</i>	100	<i>BIO3</i>	88
<i>APN1</i>	5.75E-05	2.97E-05	3.79E-03	<i>DST1</i>	98	<i>COX7</i>	88
<i>ELG1</i>	5.09E-05	1.30E-05	1.73E-04	<i>RNH202</i>	98	<i>DCS2</i>	88
<i>MLH1</i>	4.86E-05	1.15E-05	3.43E-05	<i>RNH203</i>	98	<i>DDC1</i>	88
<i>RNH203</i>	4.68E-05	6.79E-06	1.31E-05	<i>MLH1</i>	96	<i>FUS2</i>	88
<i>YLR235C</i>	4.52E-05	2.57E-06	6.11E-07	<i>NUP170</i>	96	<i>HST3</i>	88
<i>TOF1</i>	4.39E-05	1.40E-05	9.45E-04	<i>PMS1</i>	96	<i>KIP1</i>	88
<i>YAP1</i>	4.22E-05	5.04E-06	8.67E-06	<i>ALE1</i>	94	<i>MFT1</i>	88
<i>RNH202</i>	3.96E-05	1.38E-05	1.96E-03	<i>APN1</i>	94	<i>MNT2</i>	88
<i>RNH201</i>	3.86E-05	6.08E-06	1.91E-06	<i>NFI1</i>	94	<i>MRPL51</i>	88
<i>SGS1</i>	3.75E-05	1.42E-05	2.25E-03	<i>YGR117C</i>	94	<i>NIT3</i>	88
<i>YDL162C</i>	3.34E-05	9.73E-06	1.38E-03	<i>YML020W</i>	94	<i>PCL10</i>	88
<i>PMS1</i>	3.33E-05	1.28E-05	3.46E-03	<i>YMR166C</i>	94	<i>PET123</i>	88
<i>HYR1</i>	3.16E-05	1.74E-05	1.85E-02	<i>YOR072W</i>	94	<i>PHM8</i>	88
<i>MGS1</i>	3.10E-05	3.83E-06	6.14E-05	<i>RPL23a</i>	94	<i>REC114</i>	88
<i>MSH2</i>	3.09E-05	1.34E-06	1.55E-06	<i>DIA2</i>	92	<i>RGS2</i>	88
<i>DST1</i>	3.07E-05	6.56E-06	1.15E-04	<i>EFT1</i>	92	<i>SCO1</i>	88
<i>YER188W</i>	2.99E-05	1.27E-05	9.90E-03	<i>MDM1</i>	92	<i>SPR1</i>	88

<i>CSM3</i>	2.64E-05	3.65E-06	2.78E-04	<i>MSN4</i>	92	<i>TOM5</i>	88
<i>HTA2</i>	2.60E-05	6.24E-06	1.87E-03	<i>PNS1</i>	92	<i>ULS1</i>	88
<i>RAD4</i>	2.35E-05	2.46E-06	1.73E-03	<i>RMI1</i>	92	<i>YDL009C</i>	88
<i>MSH6</i>	2.34E-05	1.02E-05	1.68E-02	<i>RRT14</i>	92	<i>YEL020C</i>	88
<i>RAD6</i>	2.22E-05	7.25E-06	7.23E-03	<i>SAC3</i>	92	<i>YGL042C</i>	88
<i>RRM3</i>	2.16E-05	8.30E-06	1.54E-02	<i>YDR230W</i>	92	<i>YJL017W</i>	88
<i>CHL4</i>	2.14E-05	5.86E-06	9.36E-03	<i>YLR235C</i>	92	<i>YJR018W</i>	88
<i>THP2</i>	1.94E-05	2.95E-06	2.52E-03	<i>YNL122C</i>	92	<i>YJR124C</i>	88
<i>DFG16</i>	1.80E-05	4.48E-06	2.44E-02	<i>YTA7</i>	92	<i>YKL091C</i>	88
<i>ABZ2</i>	1.66E-05	3.93E-06	4.25E-02	<i>FSH1</i>	90	<i>YKL162C</i>	88
				<i>GET3</i>	90	<i>YNL179C</i>	88
				<i>KGD2</i>	90	<i>YOR309C</i>	88
				<i>MID2</i>	90	<i>YOR333C</i>	88
				<i>POL32</i>	90		

---

<sup>a</sup> Recombination rate from Table S2

<sup>b</sup> p-values from one-sided Student's *t*-test

**Table 2. Hypo-recombination genes from the pinning assay screen.**

Pinning Assay Hypo-Rec							
Gene name	Recombinant colonies (%)	Gene name	Recombinant colonies (%)	Gene name	Recombinant colonies (%)	Gene name	Recombinant colonies (%)
<i>YCL021W-A</i>	0.0	<i>SIP3</i>	17.2	<i>HST4</i>	27.1	<i>AIM39</i>	31.3
<i>YEL045C</i>	0.0	<i>BEM1</i>	18.8	<i>PHO85</i>	27.1	<i>CIK1</i>	31.3
<i>GLY1</i>	0.0	<i>BUB3</i>	18.8	<i>PRM4</i>	27.1	<i>HOL1</i>	31.3
<i>HIS5</i>	0.0	<i>OPI3</i>	18.8	<i>RIM1</i>	27.1	<i>MET22</i>	31.3
<i>RAD52</i>	2.1	<i>YER038W-A</i>	18.9	<i>UBP15</i>	27.1	<i>SWH1</i>	31.3
<i>GCN4</i>	2.9	<i>ARG7</i>	19.1	<i>VMA21</i>	27.1	<i>RNR4</i>	31.3
<i>CYS4</i>	3.1	<i>LIN1</i>	19.6	<i>YBR075W</i>	27.1	<i>RPN4</i>	31.3
<i>POS5</i>	3.1	<i>OPY2</i>	20.0	<i>AAT2</i>	27.5	<i>RPS18B</i>	31.3
<i>REC104</i>	4.2	<i>HEF3</i>	20.0	<i>RAD50</i>	27.8	<i>TSL1</i>	31.3
<i>YHR080C</i>	4.2	<i>DAL81</i>	20.9	<i>ARG2</i>	28.1	<i>VPS60</i>	31.3
<i>ATP15</i>	4.8	<i>YLR361C-A</i>	21.3	<i>IRE1</i>	28.2	<i>VTH1</i>	31.3
<i>YPR099C</i>	4.9	<i>RPL22A</i>	21.6	<i>PDR16</i>	28.2	<i>YKE2</i>	31.3
<i>YOR302W</i>	5.3	<i>RSM7</i>	21.7	<i>RNR1</i>	28.2	<i>YNR040W</i>	31.3
<i>ACO2</i>	6.4	<i>CCR4</i>	22.2	<i>YKR023W</i>	28.6	<i>NUP84</i>	31.6
<i>MDM20</i>	6.4	<i>LOC1</i>	22.2	<i>ATP1</i>	29.2	<i>BOI1</i>	31.7
<i>MDM10</i>	6.9	<i>AHC1</i>	22.9	<i>FIT2</i>	29.2	<i>URA2</i>	31.7
<i>NPL3</i>	7.1	<i>CIN1</i>	22.9	<i>HSP42</i>	29.2	<i>RTC3</i>	31.8
<i>HIS7</i>	7.7	<i>VRP1</i>	22.9	<i>RAD54</i>	29.2	<i>THP1</i>	31.8
<i>FUN12</i>	8.3	<i>YEL014C</i>	22.9	<i>RAD55</i>	29.2	<i>BUD20</i>	32.1
<i>BDF1</i>	11.1	<i>CDC40</i>	23.1	<i>SNO1</i>	29.2	<i>RPS16A</i>	32.6
<i>YNL011C</i>	12.5	<i>MDM34</i>	23.4	<i>SPE2</i>	29.2		
<i>SWI6</i>	12.8	<i>OST4</i>	23.5	<i>SPT21</i>	29.2		
<i>URA1</i>	13.2	<i>YOL013W-B</i>	24.0	<i>TCD1</i>	29.2		
<i>YGR272C</i>	13.2	<i>YCK1</i>	24.3	<i>TPM1</i>	29.2		

<i>BUD19</i>	13.3	<i>KNH1</i>	25.0	<i>YDR157W</i>	29.2
<i>UGO1</i>	13.3	<i>SHE4</i>	25.0	<i>YDR535C</i>	29.2
<i>YBL065W</i>	14.6	<i>SNF6</i>	25.0	<i>YNL097C-A</i>	29.2
<i>SWI3</i>	14.8	<i>YDL187C</i>	25.0	<i>YME1</i>	29.6
<i>BRE4</i>	15.2	<i>LRP1</i>	25.7	<i>NGG1</i>	30.3
<i>YGR139W</i>	15.6	<i>ACM1</i>	25.9	<i>POP2</i>	30.4
<i>PMD1</i>	15.8	<i>VCX1</i>	26.7	<i>ATP11</i>	30.8
<i>YHL041W</i>	15.8	<i>BUB1</i>	26.8	<i>RPL37B</i>	31.0
<i>ERG28</i>	16.7	<i>CCW12</i>	27.1	<i>HFI1</i>	31.0
<i>SLX5</i>	16.7	<i>HAM1</i>	27.1	<i>YML013C-A</i>	31.1

---

**Table 3. Validated hyper-recombination genes from the patch assay and pinning assay screens.**

<b>Gene name</b>	<b>Description</b>	<b>Human orthologue(s)</b>
<i>HTA2</i>	Histone H2A	H2A
<i>NUP170</i>	Subunit of inner ring of nuclear pore complex	NUP155
<i>CSM1</i>	Nucleolar protein that mediates homolog segregation during meiosis I	
<i>YDL162C</i>	Dubious open reading frame; overlaps the CDC9 promoter	LIG1
<i>MSH6</i>	Protein required for mismatch repair in mitosis and meiosis	MSH6
<i>CHL4</i>	Outer kinetochore protein required for chromosome stability	CENPN
<i>RNH202</i>	Ribonuclease H2 subunit	RNASEH2B
<i>RAD4</i>	Protein that recognizes and binds damaged DNA during NER	XPC
<i>YER188W</i>	Putative protein of unknown function	
<i>DST1</i>	General transcription elongation factor TFIIIS	TCEA1, TCEA2, TCEA3
<i>RAD6</i>	Ubiquitin-conjugating enzyme	UBE2A, UBE2B
<i>RRM3</i>	DNA helicase involved in rDNA replication and Ty1 transposition	PIF1
<i>THP2</i>	Subunit of the THO and TREX complexes	
<i>SKN7</i>	Nuclear response regulator and transcription factor	HSF1, HSF2, HSF4, HSF5
<i>HYR1</i>	Thiol peroxidase	GPX1, GPX2, GPX3, GPX4, GPX5, GPX6, GPX7
<i>RAD27</i>	5' to 3' exonuclease, 5' flap endonuclease	FEN1
<i>APN1</i>	Major apurinic/apyrimidinic endonuclease	APE1

<i>RNH203</i>	Ribonuclease H2 subunit	RNASEH2C
<i>TOP3</i>	DNA Topoisomerase III	TOP3A
<i>YLR235C</i>	Dubious open reading frame; overlaps the TOP3 gene	TOP3A
<i>YAP1</i>	Basic leucine zipper transcription factor	
<i>TSA1</i>	Thioredoxin peroxidase	PRDX1, PRDX2, PRDX3, PRDX4
<i>CSM3</i>	Replication fork associated factor	TIPIN
<i>MLH1</i>	Protein required for mismatch repair in mitosis and meiosis	MLH1
<i>SGS1</i>	RecQ family nucleolar DNA helicase	BLM
<i>ABZ2</i>	Aminodeoxychorismate lyase (4-amino-4-deoxychorismate lyase)	
<i>RNH201</i>	Ribonuclease H2 catalytic subunit	RNASEH2A
<i>PMS1</i>	ATP-binding protein required for mismatch repair	PMS1
<i>MGS1</i>	Protein with DNA-dependent ATPase and ssDNA annealing activities	WRNIP1
<i>TOF1</i>	Subunit of a replication-pausing checkpoint complex	TIMELESS
<i>MSH2</i>	Protein that binds to DNA mismatches	MSH2
<i>DFG16</i>	Probable multiple transmembrane protein	
<i>ELG1</i>	Subunit of an alternative replication factor C complex	ATAD5
<i>RMI1</i>	Subunit of the RecQ (Sgs1) - Topo III (Top3) complex	RMI1
<i>VMA11</i>	Vacuolar ATPase V0 domain subunit c'	ATP6VOC

---